Research and application of marine atmospheric boundary layer taken in part of the South China Sea

Reporter: Zhao Zhongkuo

Guangzhou Institute of Tropical and Marine Meteorology, China Meteorological Administration

2023-11-27 9:00-10:30

The 8th International Training Course on Typhoon Operations

How many of you have oceanography background?

contents

Schematic of the marine-atmospheric boundary layer

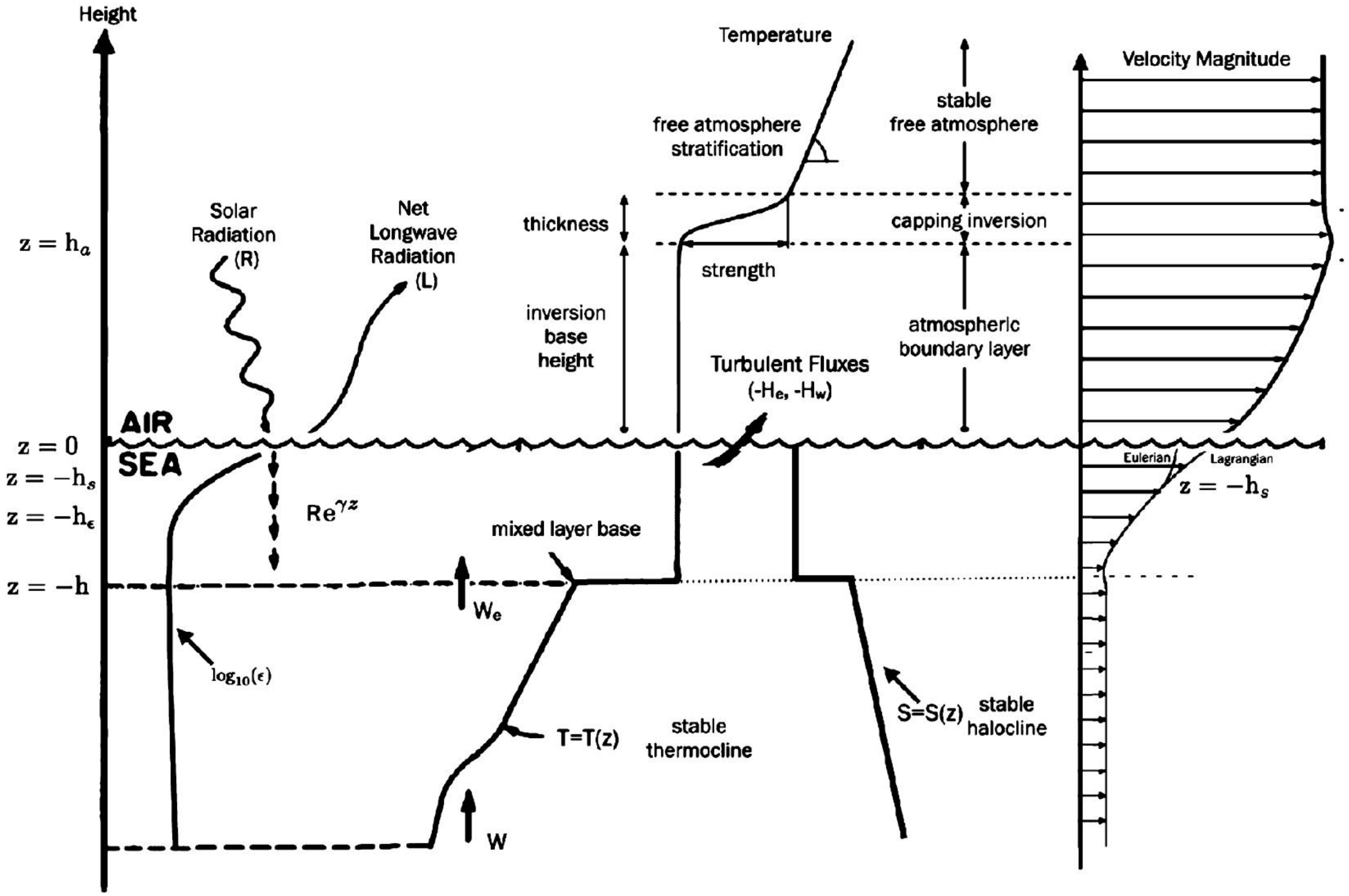

Courtesy of Meredith and Garabato (2021)

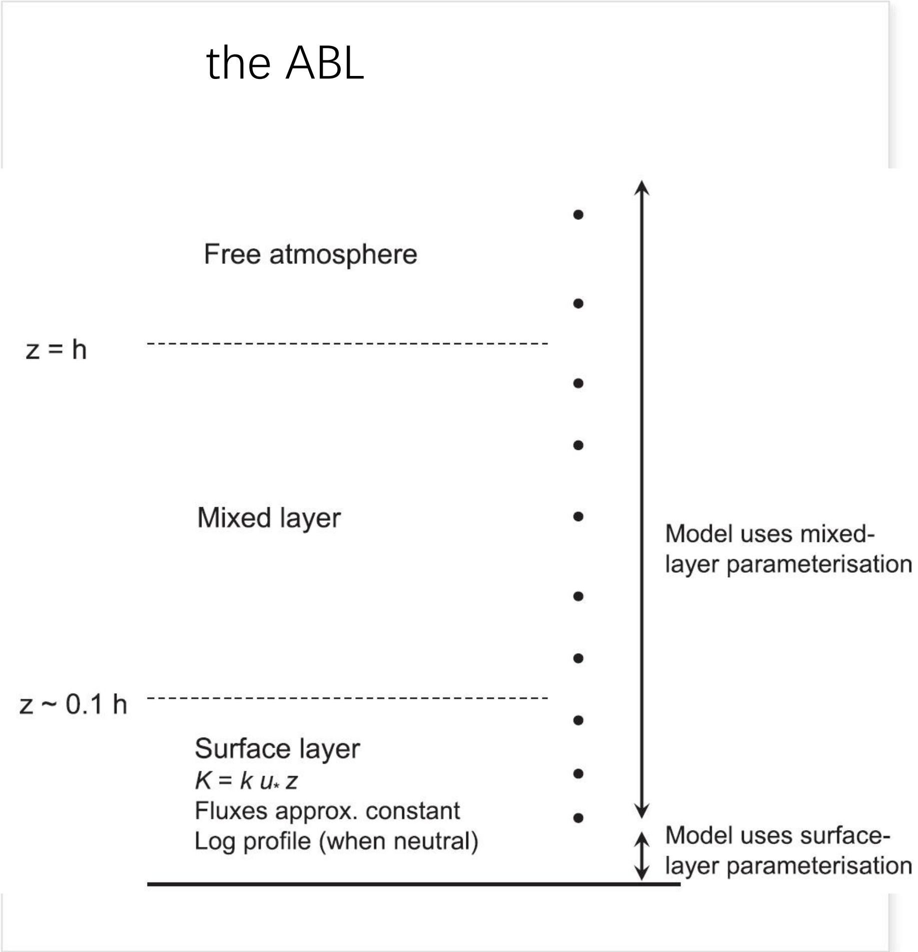

Courtesy of Kepert (2012)

Air-sea interface: a typical example of flow-wave interaction

- Parameter space of the problem can be partitioned into 3 regimes:
(Sullivan and McWilliams, 2010)
  - ✓ Wave age c/U<1.2: wind-driven wave
  - ✓ Wave age c/U>1.2: wave-driven wind
  - ✓ Wave age c/U~1.2: wave-wind equilibrium
- The typical wave boundary layer height is

$$H_{WBL} \sim k_p^{-1}$$

where k_p is the peak wavenumber (Chalikov, 1995)

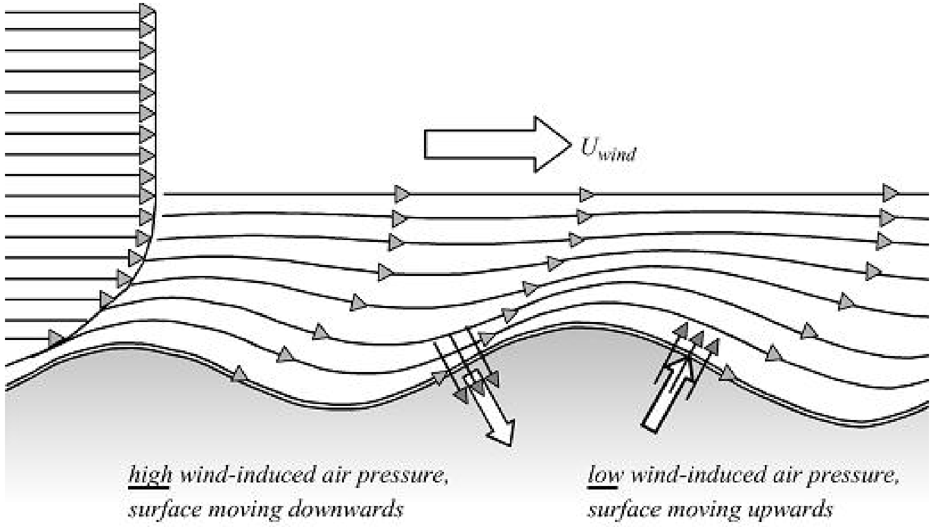

Courtesy of Holthuijsen (2007)

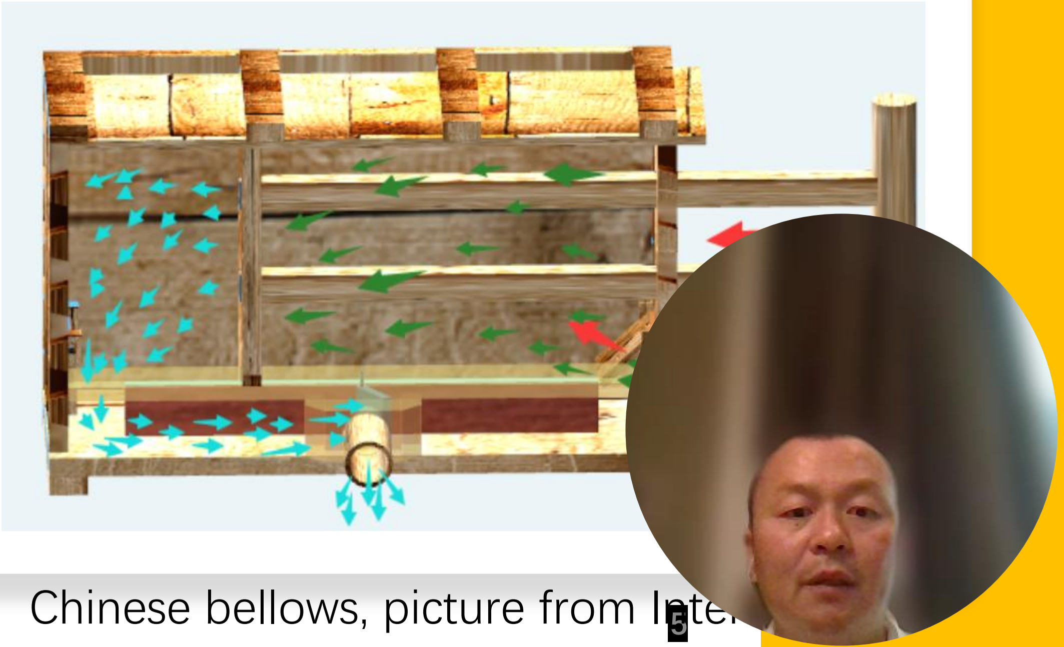

Chinese bellows, picture from Inte

Part 1 Marine atmospheric surface-layer momentum fluxes and its parameterization during typhoon

1. Background
2. Observations
3. results and analysis
4. Preliminary application

Reference: Zhao, Zhong Kuo, Chun Xia Liu, Qi Li, Guang Feng Dai, Qing Tao Song and Wei Hua Lv (2015). Typhoon air-sea drag coefficient in coastal regions. Journal of Geophysical Research: Oceans 120(2): 716–727.

AGU Publications
https://agupubs.onlinelibrary.wiley.com › full · 翻译此页

Typhoon air-sea drag coefficient in coastal regions - Zhao

作者：ZK Zhao · 2015 · 被引用次数：71 — The drag coefficient (CD) plotted against the typhoon wind speed is similar to that of open ocean conditions; however, the CD curve shifts ...

Abstract · Introduction · Measurements and Data... · Results and Discussion

Background: Field observations in hurricanes

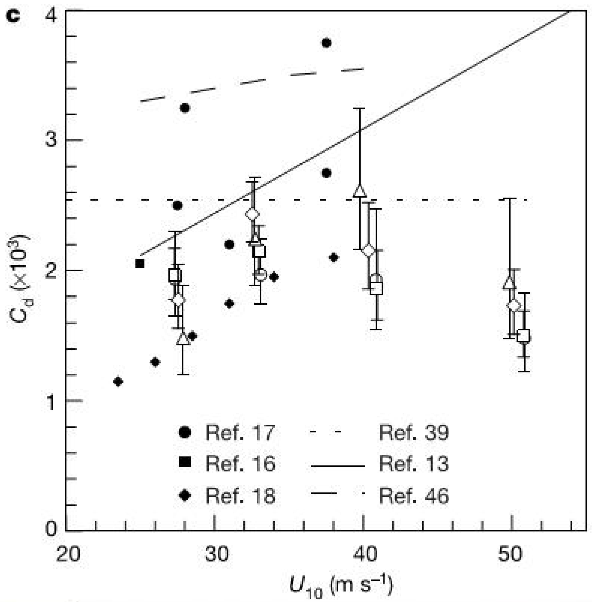

Nature, 2003

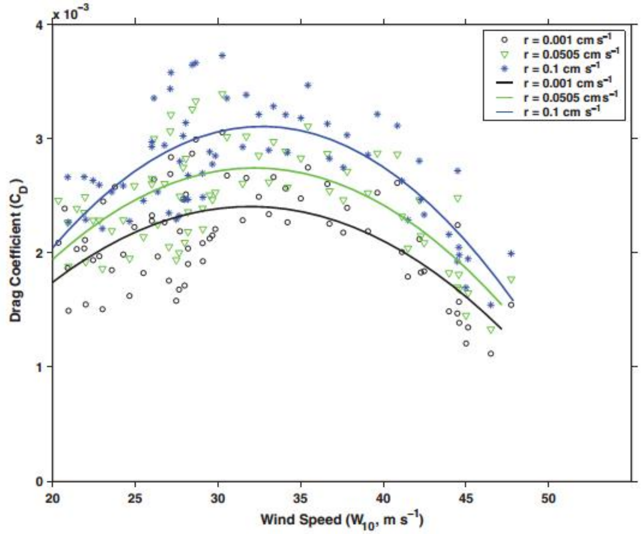

Science, 2007

Holthuijsen et al, 2012, JGR

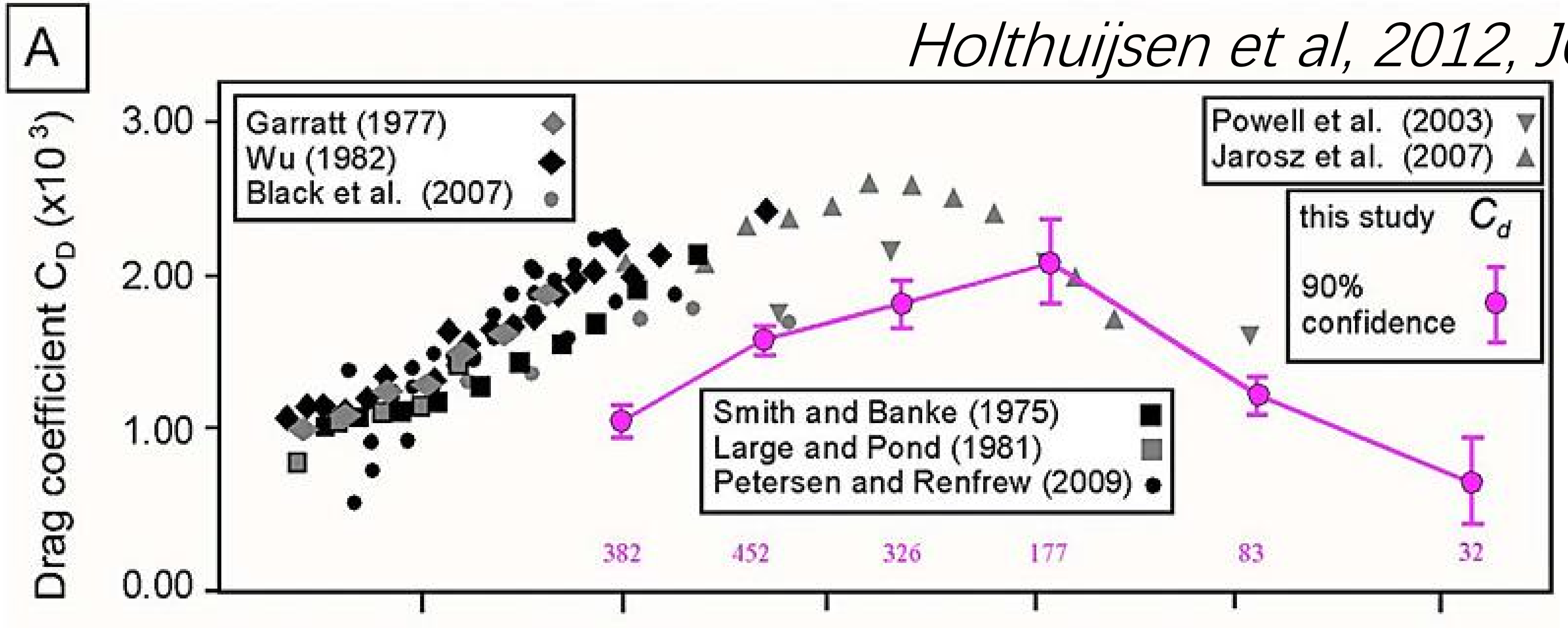

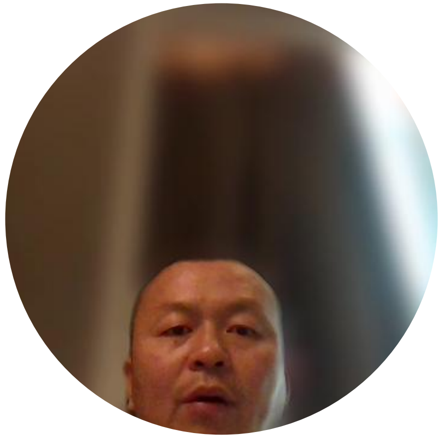

Background: laboratory experiments

Alamaro, et al, 2001

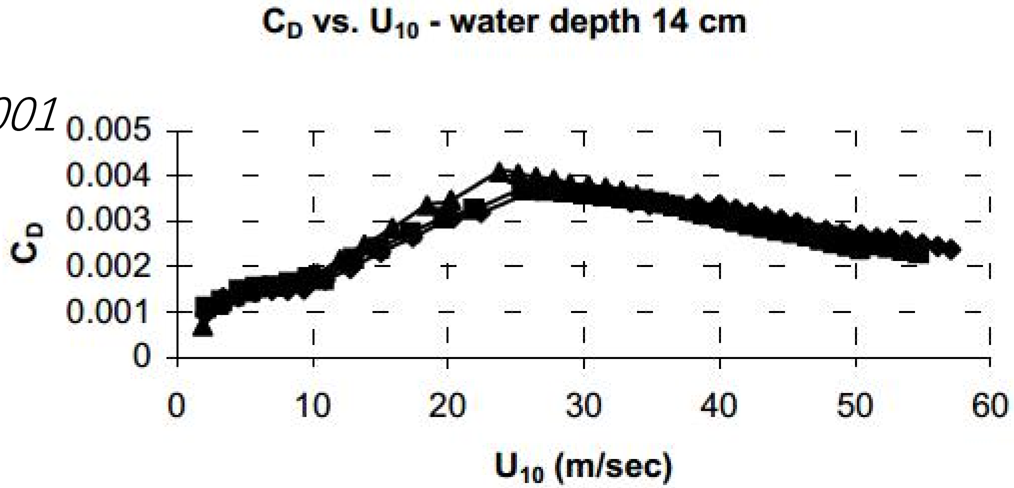

Donelan et al, 2004

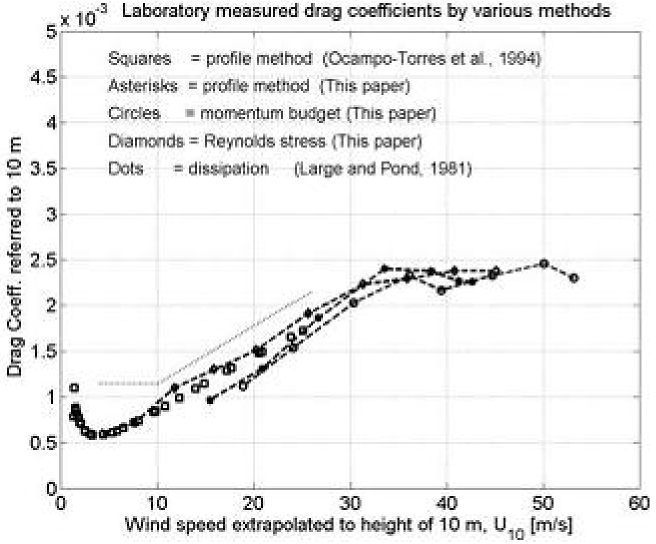

Troitskaya et al, 2012

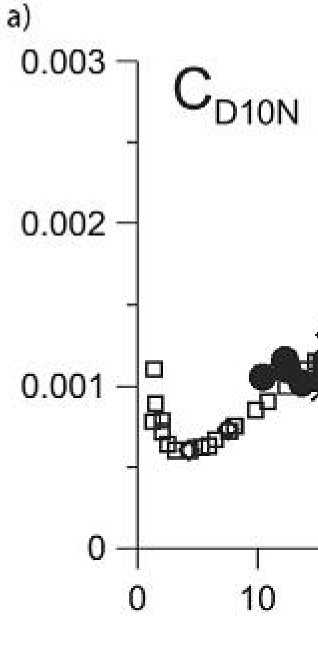

Background-theoretical study

Liu et al, 2012

$$\frac{gz_0}{u_*^2} = \begin{cases} c_l^{1-1/\omega}[0.03\beta_* \exp(-0.14\beta_*)]^{1/\omega}, & \sim 0.35 < \beta_* < 35 \\ c_l^{1-1/\omega}(0.008)^{1/\omega}, & \beta_* \geq 35 \end{cases}$$

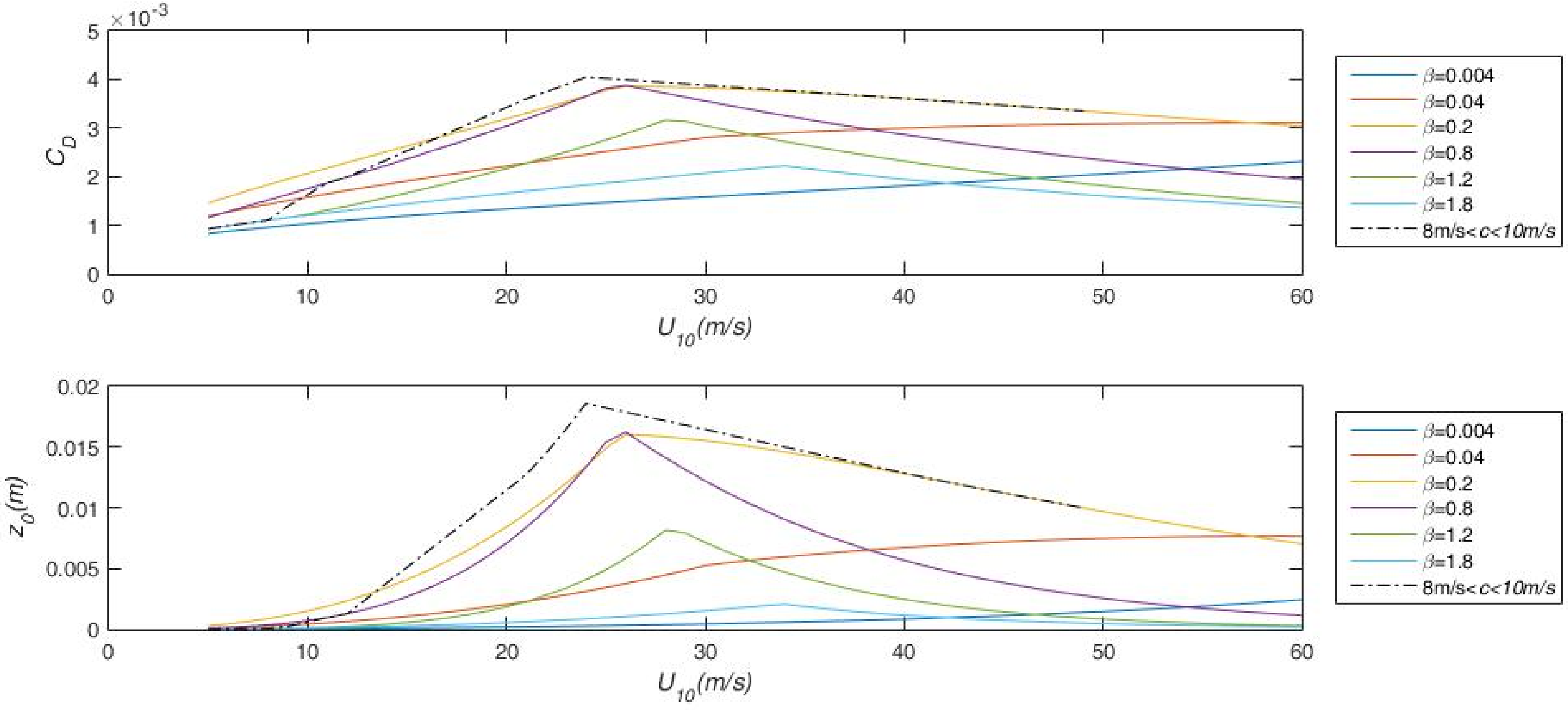

Motivation

- These observed drag coefficients at high wind speeds have been incorporated into the atmosphere, ocean and wave models, e.g., improving the prediction of typhoon structures and track, waves, storm surge, etc.
- Previous research on the impact of shoaling waves on air-sea momentum flux found that at the same wind speed, the drag coefficient over shallow water is higher than that in the deep ocean. However, the maximum wind speed of these results does not exceed 20 m/s.
- This study is based on observations in coastal water during typhoons and focuses on the impact of shoaling waves on air-sea momentum exchange.

2 Observations-at a coastal tower in the SCS during 2 typhoons

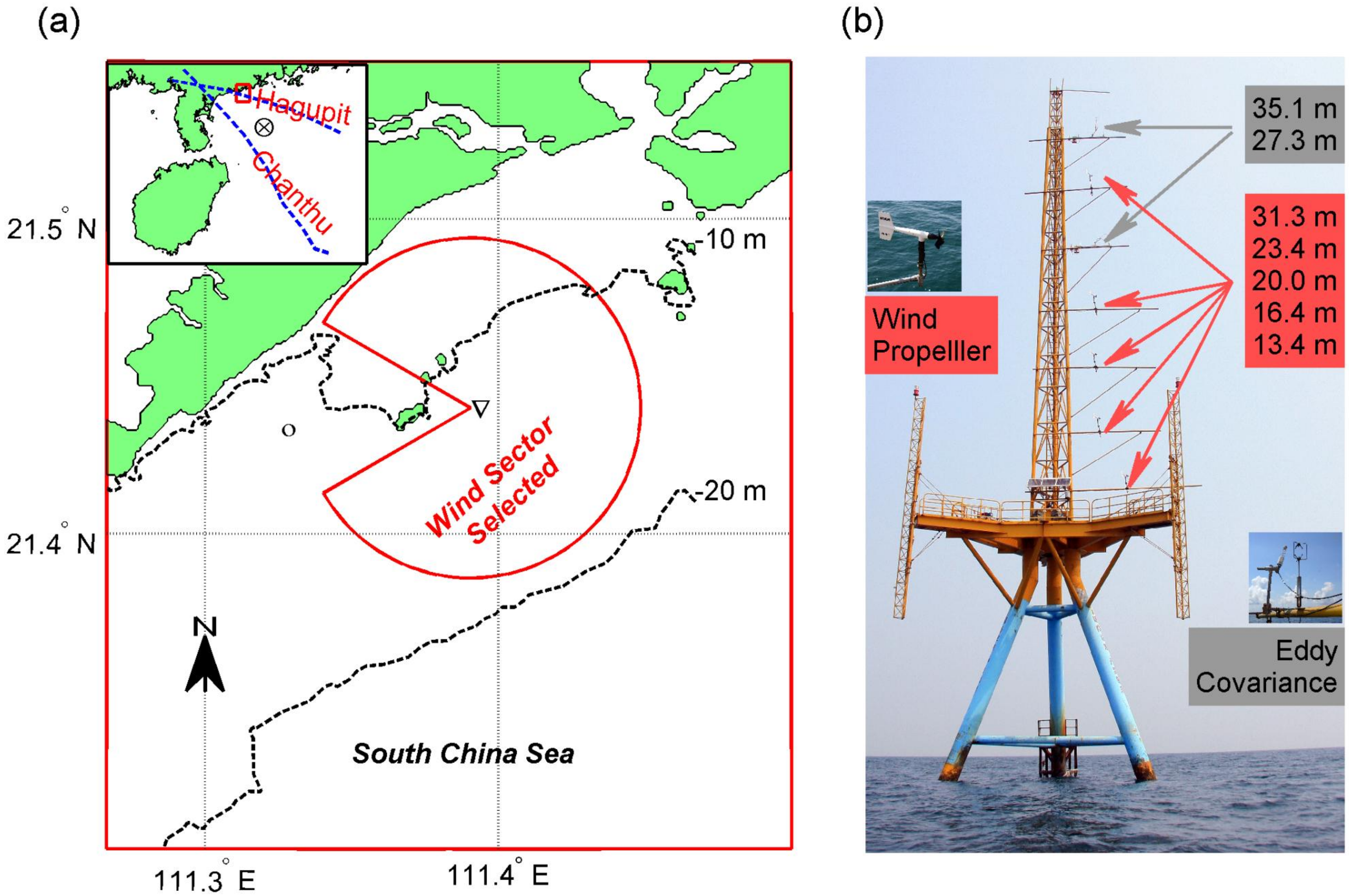

Observations-data timeseries during typhoon Hagupit(2008)

Corresponding to the selected wind speed, an average significant wave period (conserved quantity) is obtained as 9.3 s.

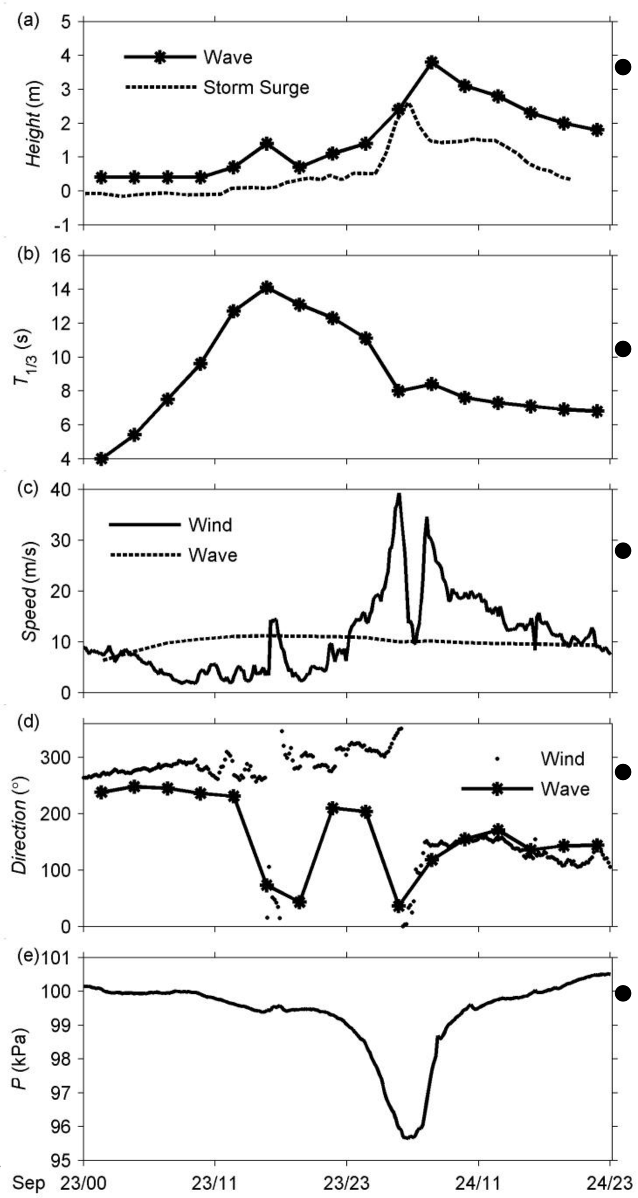

- Wave height $H_{1/3}$ and storm surge η
- Wave period $T_{1/3}$
- Wind/Wave speed *U, c*
- Wind/Wave *Direction*
- Atmosphere *Pressure*

Observations-method (wind speed - logarithmic height)

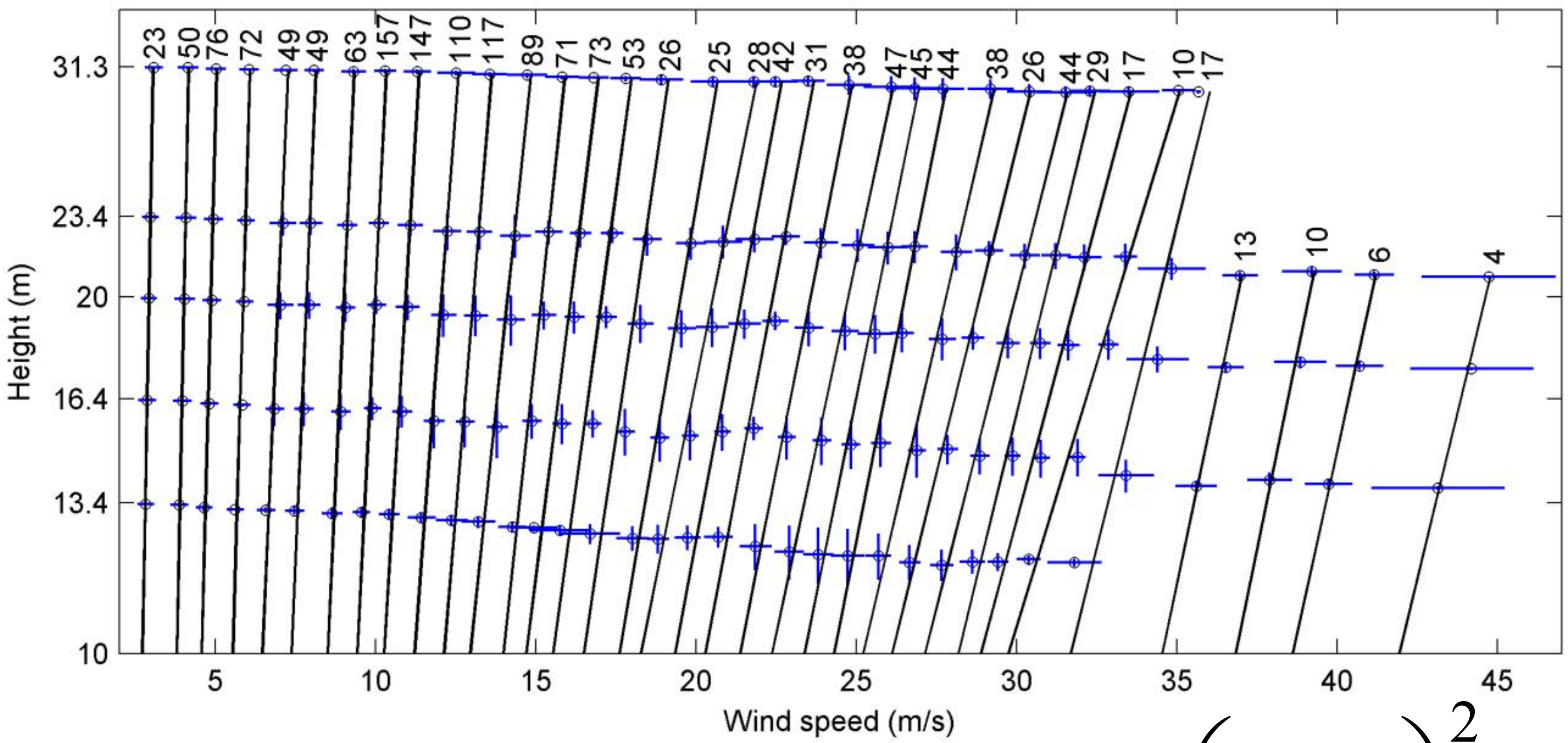

$$U_z = \frac{u_*}{k}\ln\left(\frac{z}{z_0}\right) \qquad C_D = \left(\frac{u_*}{U_{10}}\right)^2$$

Results – Dependence of friction velocity and drag coefficient on wind speed

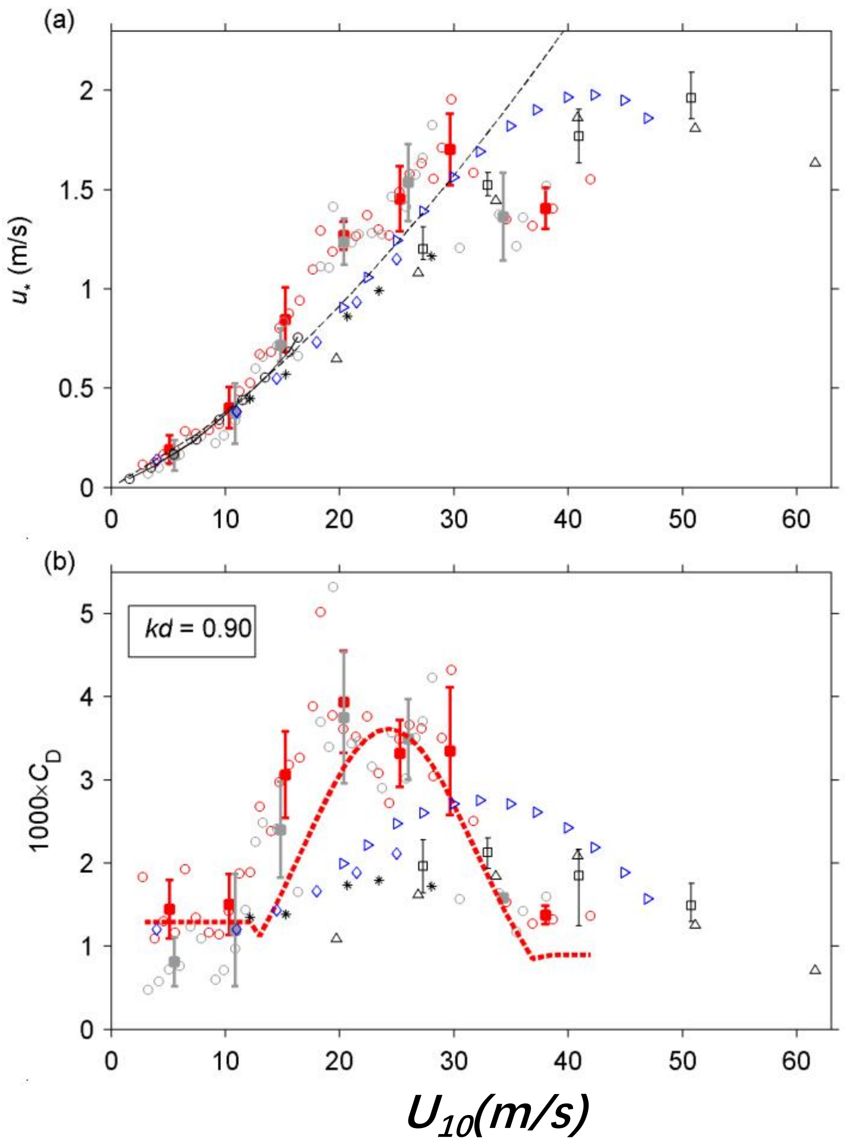

Only the field observation results were compared.

kd: dimensionless depth

Red & Gray: Results in this article (shallow water, *kd*=0.9)

- Blue: results from medium depth(*kd*=2.33)
- Black: open ocean, infinite water depth

Explanations

- The reduction of drag coefficient in high winds corresponding to sea surface wave breaking and smoothing.
- The shallower the water, the steeper the waves and the easier they are to break, causing the maximum drag coefficient to appear at smaller wind speeds.
- Effective waves are selected for analysis, water depth is used as a parameter to characterize sea conditions, and a drag coefficient parameterization scheme that relies on water depth and wind speed is developed.

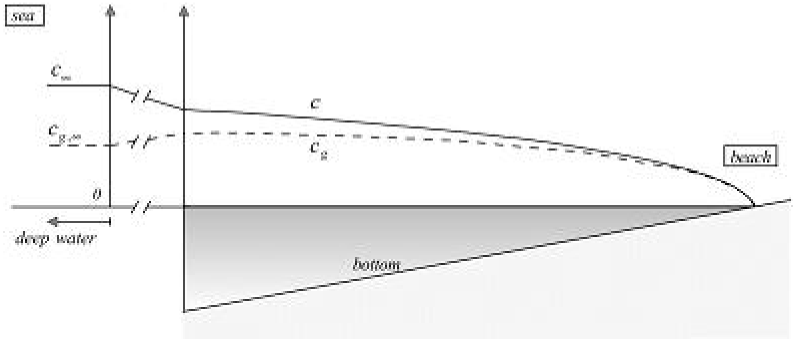

Variations of wave phase speed and group velocity as approaching coast

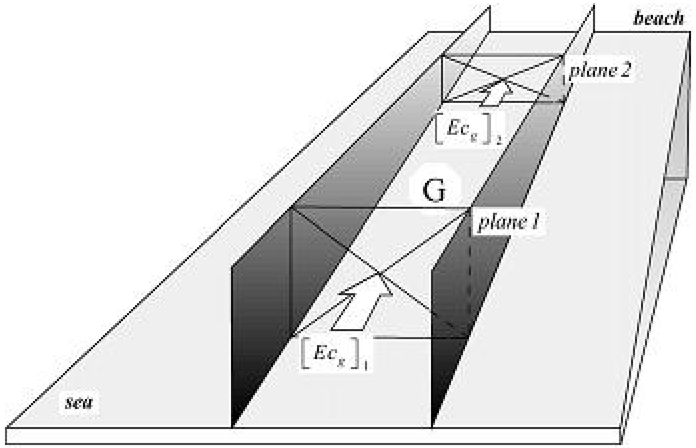

Amplitude evolution due to shoaling

Shoaling wave effects, Courtesy of Holthuijsen (2007)

Steps of the parameterization

$$C_D = C_D\left(\frac{U_{10}}{(gz_1)^{1/2}}, \frac{gd}{U_{10}^2}, \frac{U_{10}}{c}, S\right)$$

1. Fitting with the open ocean results

$$1000\times C_D = -1.85\tilde{u}^2 + 3.70\tilde{u} - 0.05$$

$$\tilde{u} = U_{10}/U_{ref}, U_{ref} = U_{10c\infty} = 34m/s$$

2. $$r_{slope} = \frac{ka}{k_\infty a_\infty} = \frac{k}{k_\infty}\times\sqrt{\frac{c_{g\infty}}{c_g}}$$

3. $$U_{ref} = \frac{U_{10c\infty}}{r_{slope}}$$

4. $$1000\times C_D = \max\left\{\frac{\hbar}{b+\tanh\left(\frac{gd}{u_{c\infty}^2}\right)^b}, \frac{\exp\left[-\frac{(U_{10}-u_{ref})^2}{gd}\right]}{\tanh\left(\frac{gd}{u_{c\infty}^2}\right)^b}(p(1)\tilde{u}^2 + p(2)\tilde{u} + p(3))\right\}$$

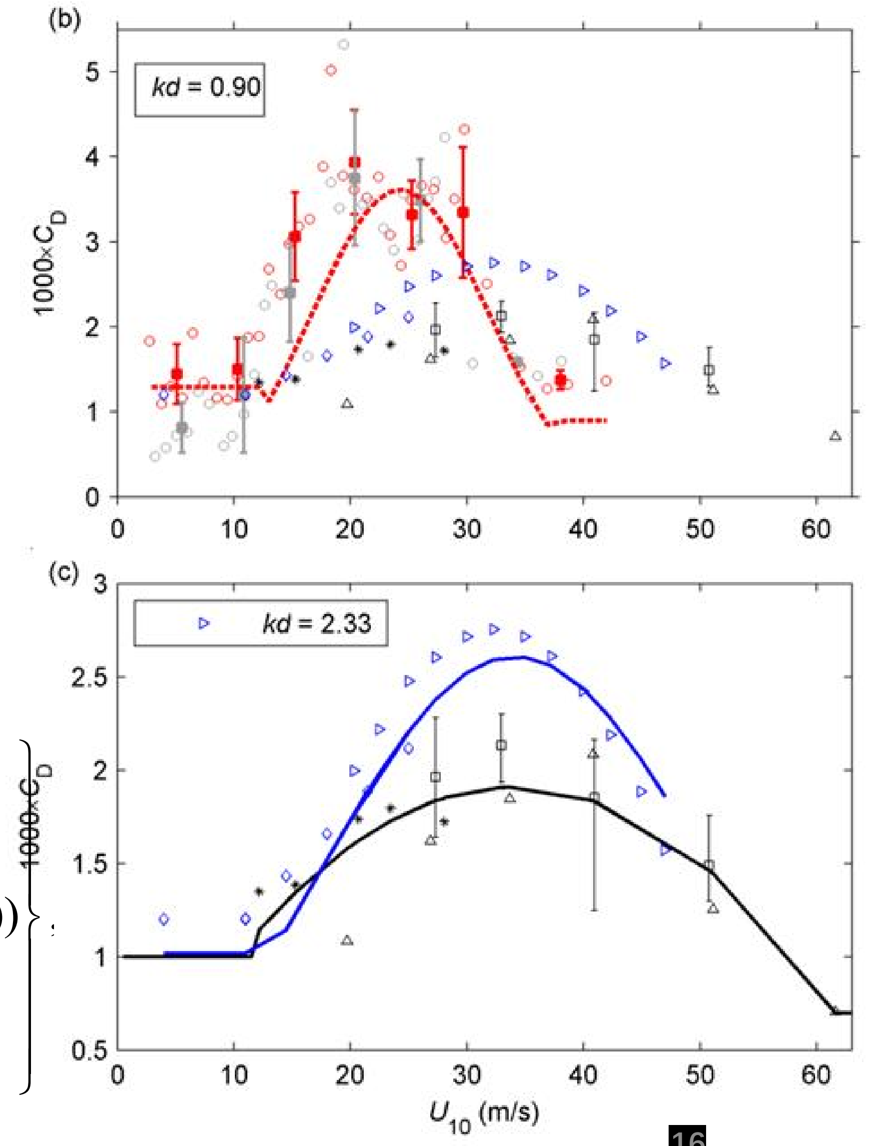

Application-case of typhoon Nanmadol (2011)

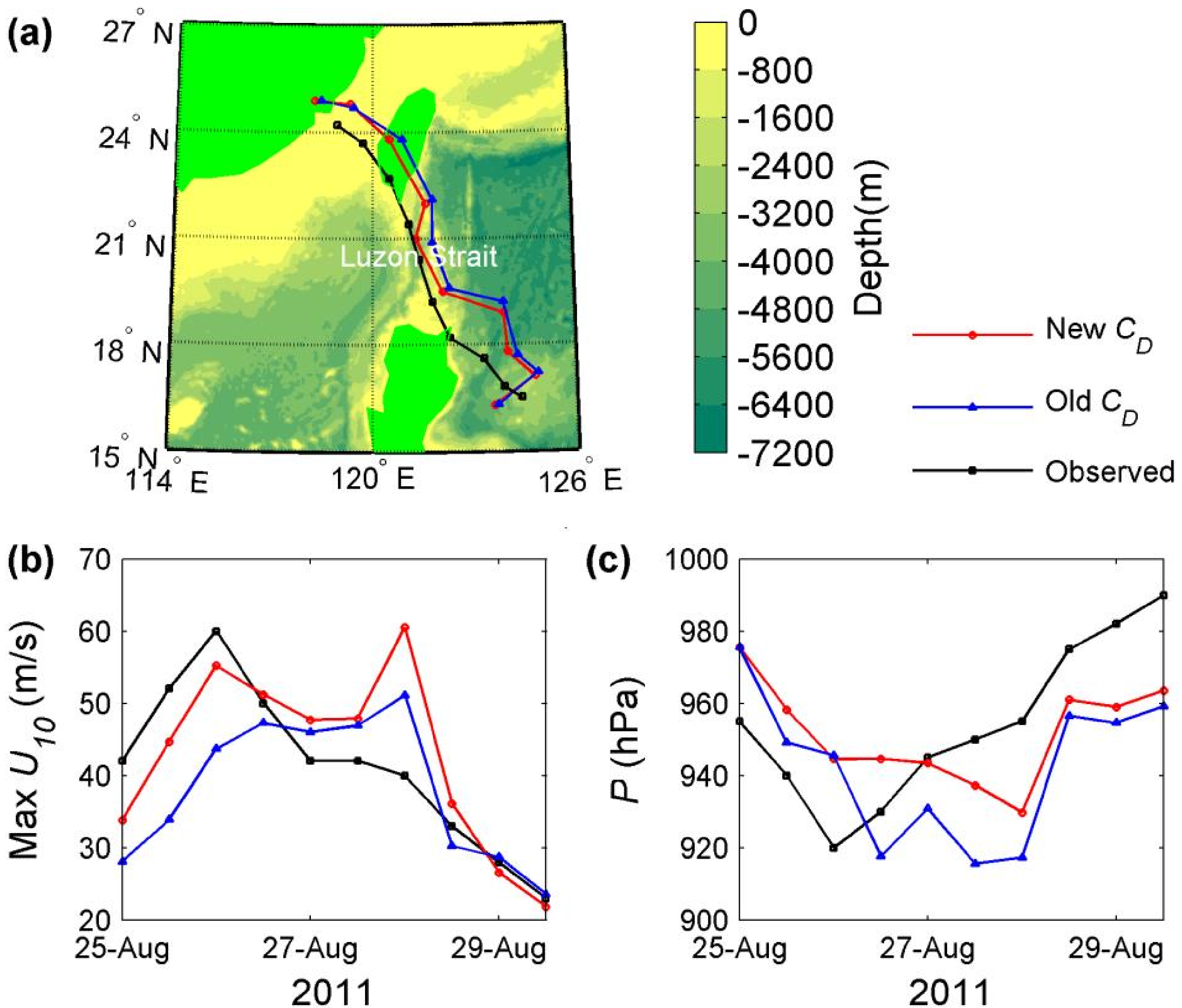

Application-

- Batch test for all the typhoons in 2012

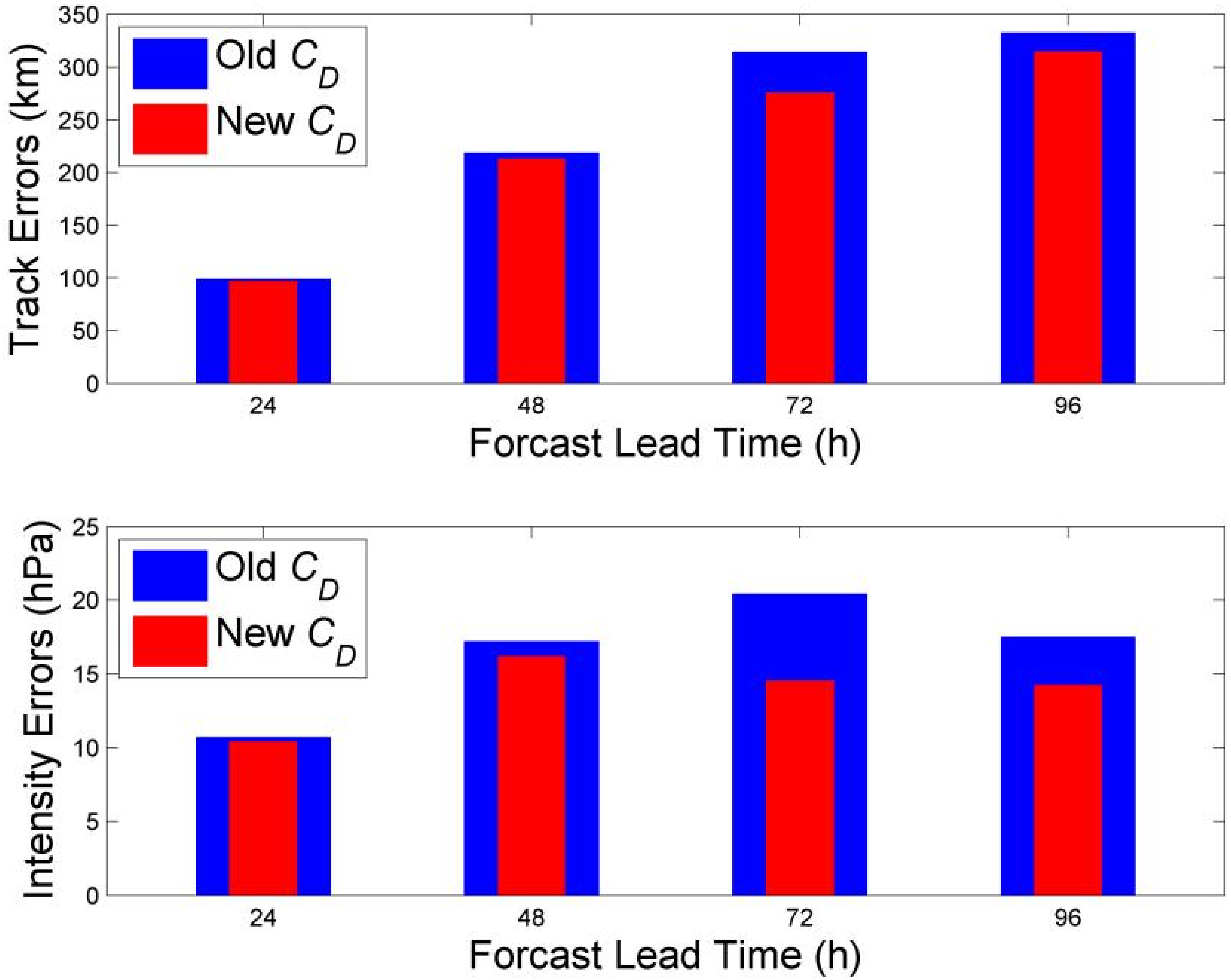

Conclusions

- Compared with the observation results in deep water areas and medium water depth areas, the typhoon air-sea momentum flux and drag coefficient observed in the shallow water area of the Bohe Marine Meteorological Platform have significantly different performances, especially the critical wind speed corresponding to when the drag coefficient reaches the maximum value.
- The shoaling wave effect can explain the differences in observation results under different water depth conditions.
- A parameterization scheme for drag coefficient that depends on water depth and wind speed is proposed. Individual case and batch test results show that the new scheme has a positive effect on typhoon forecasting

Part2-Effects of underlying wavy surface

Reference

Huang, Jian, Zhongshui Zou, Qingcun Zeng, Peiliang Li, Jinbao Song, Lin Wu, Jun A. Zhang, Shuiqing Li and Pak-wai Chan (2021). The Turbulent Structure of the Marine Atmospheric Boundary Layer during and before a Cold Front %J Journal of the Atmospheric Sciences. 78(3): 863-875.

Attached Eddy Model(AEM)

The inertial-dominated logarithmic region of eddies is a focus of wall turbulence study recently.

AEM, proposed by Townsend, depicts the wall turbulence complex physics in terms of simple geometrically self-similar attached eddies, and is supposed to be ideally suited for describing and assessing atmospheric surface layer flows.

Based on AEM, the horizontal velocity variances are expected to be logarithmic with height, and the vertical velocity variance is independent on height

$$\frac{\overline{u'^2_i}}{u_*^2} = B_1 - A_1 \ln\left(\frac{z}{\delta}\right), \quad i = 1, 2; \qquad (1)$$

$$\frac{\overline{u'^2_i}}{u_*^2} = B_2, \quad i = 3, \qquad (2)$$

Part 2-test of AEM over coast sea

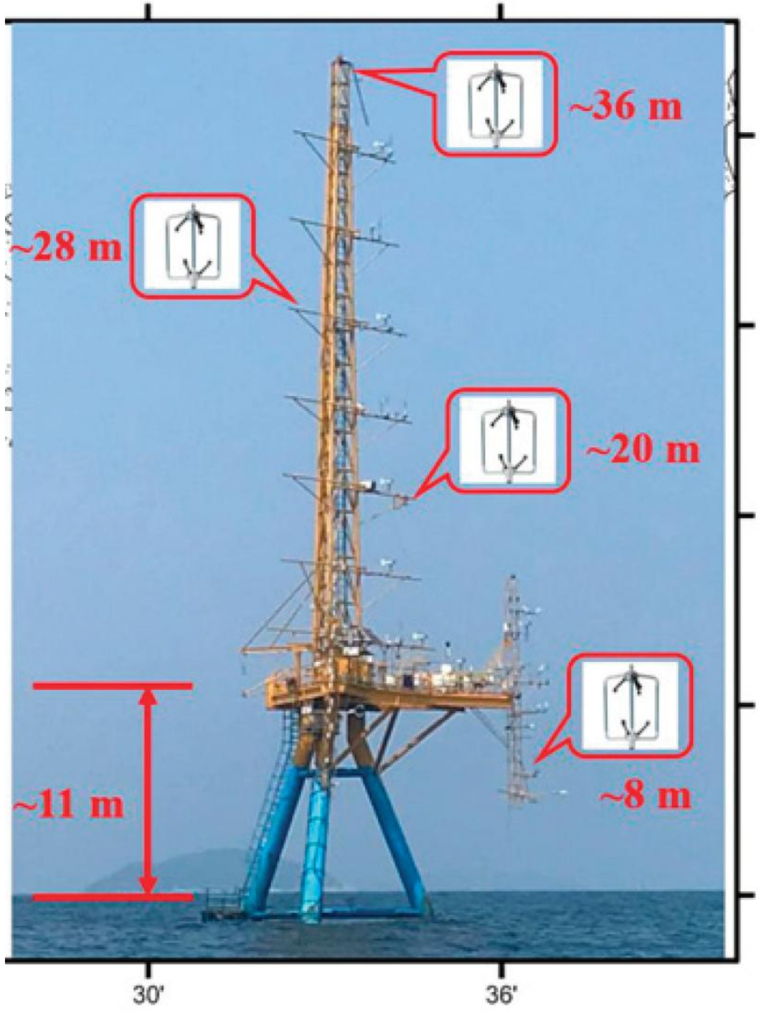

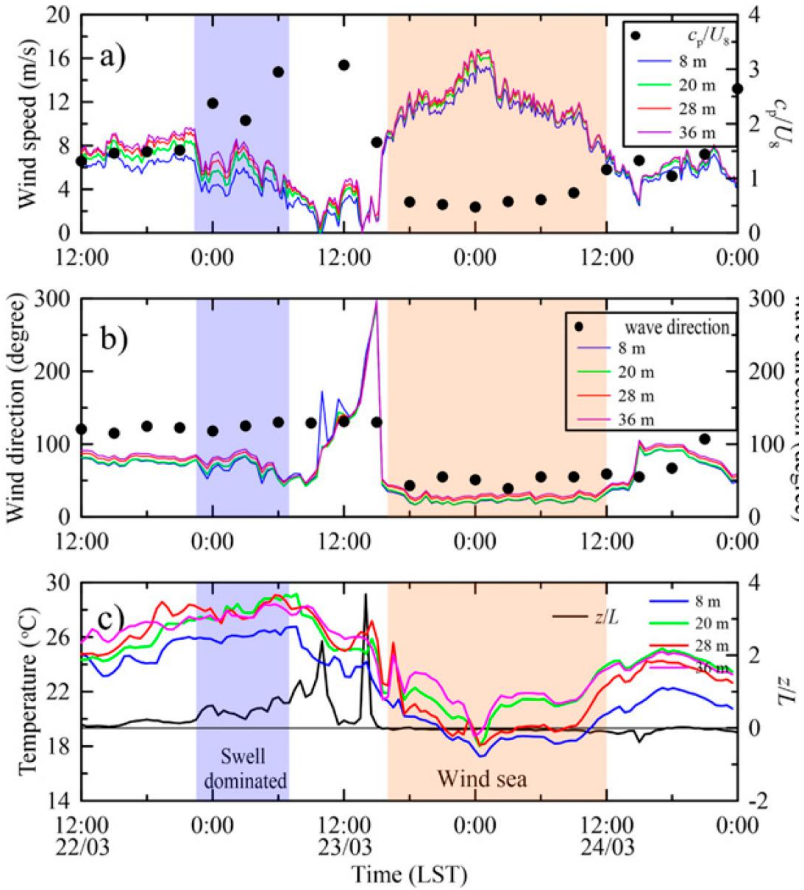

Huang J. et al, 2021

Part 2-test of wall turbulence attached eddy model in cases of windsea and swell

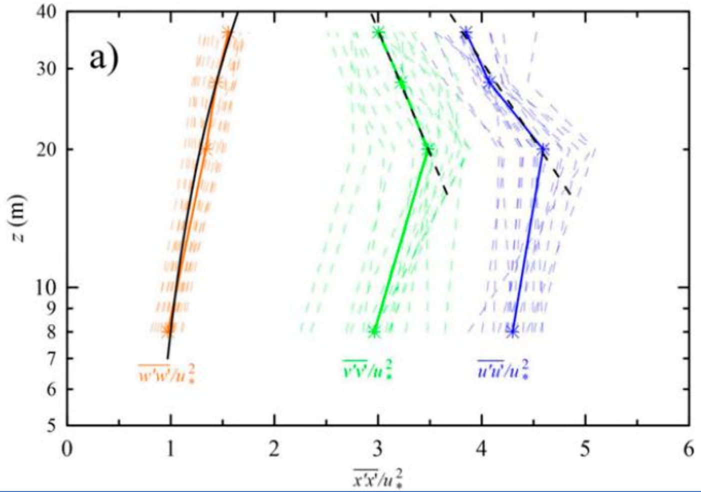

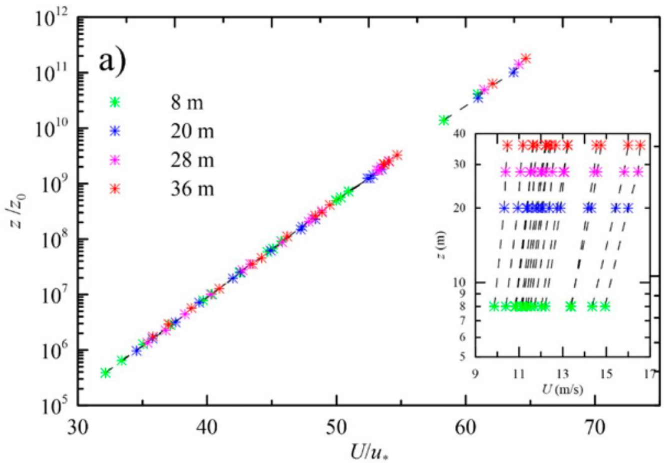

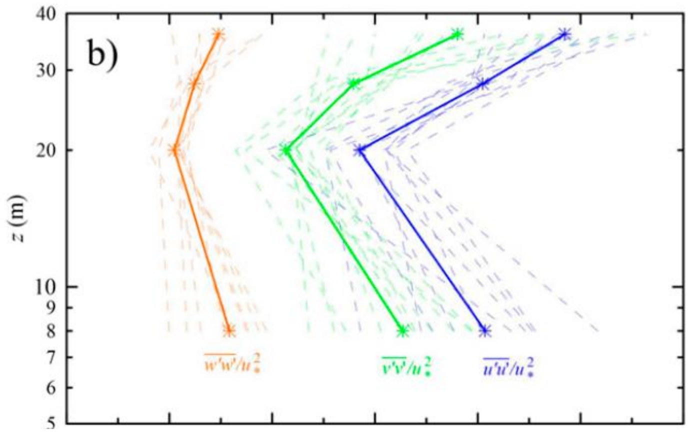

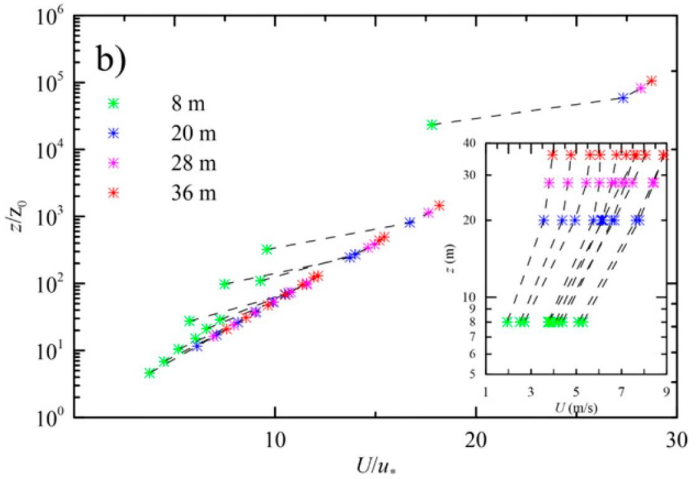

- (upper)Windsea: the 3 velocity variances follow AEM roughly, which means eddies attached to the windsea surface and 'top-down' turbulence
- (lower)Swell: the 3 velocity variances deviate from AEM significantly in the wave boundary layer

Part 3-Marine Atmospheric mixed-layer observations during typhoon

Reference

Zhao, Zhongkuo, P. W. Chan, Naigeng Wu, Jun A. Zhang and K. K. Hon (2020). Aircraft Observations of Turbulence Characteristics in the Tropical Cyclone Boundary Layer. Boundary-Layer Meteorology 174(3): 493-511.

Contents

- Background
- Data and methods
- Result analysis
- Discussion and conclusion

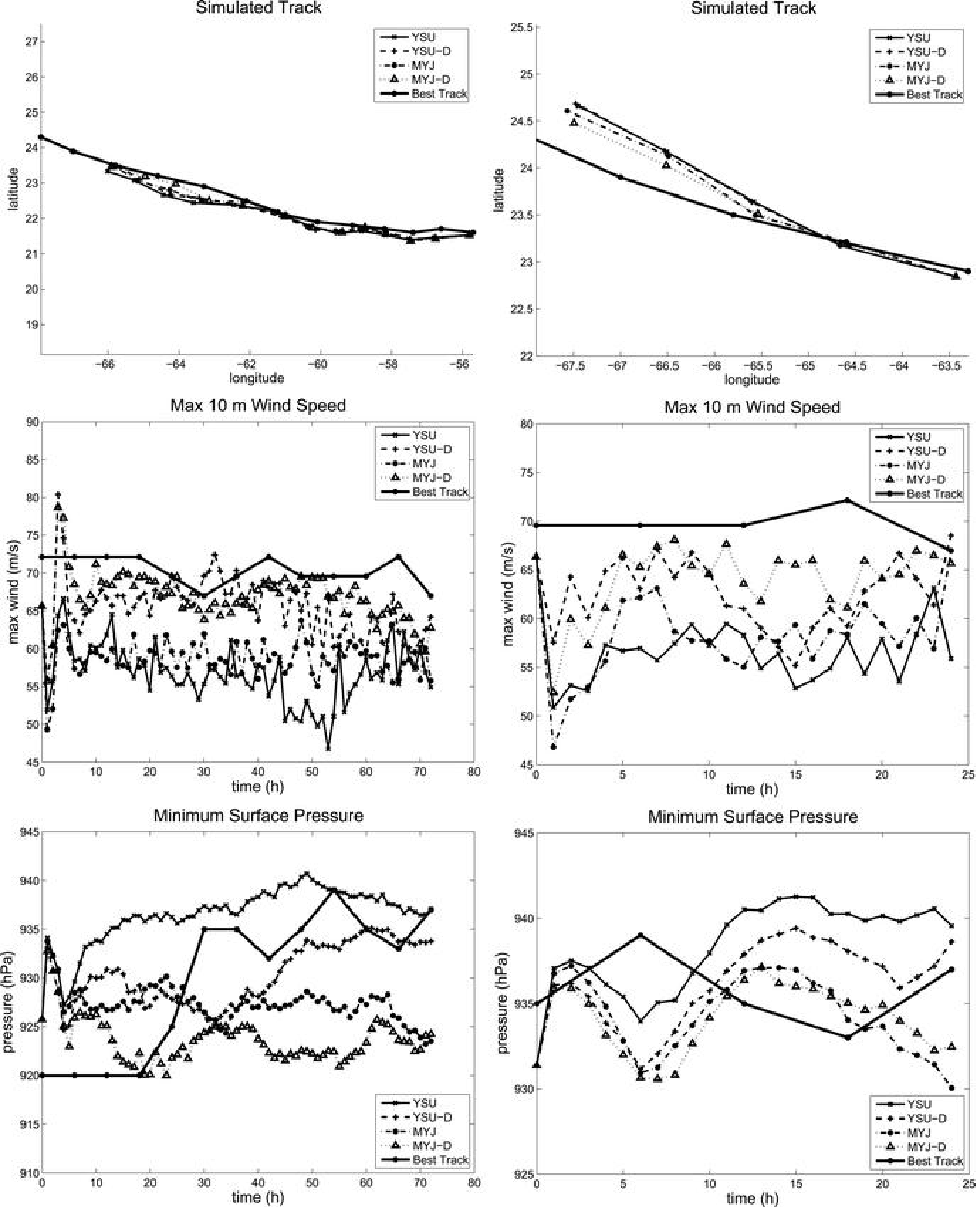

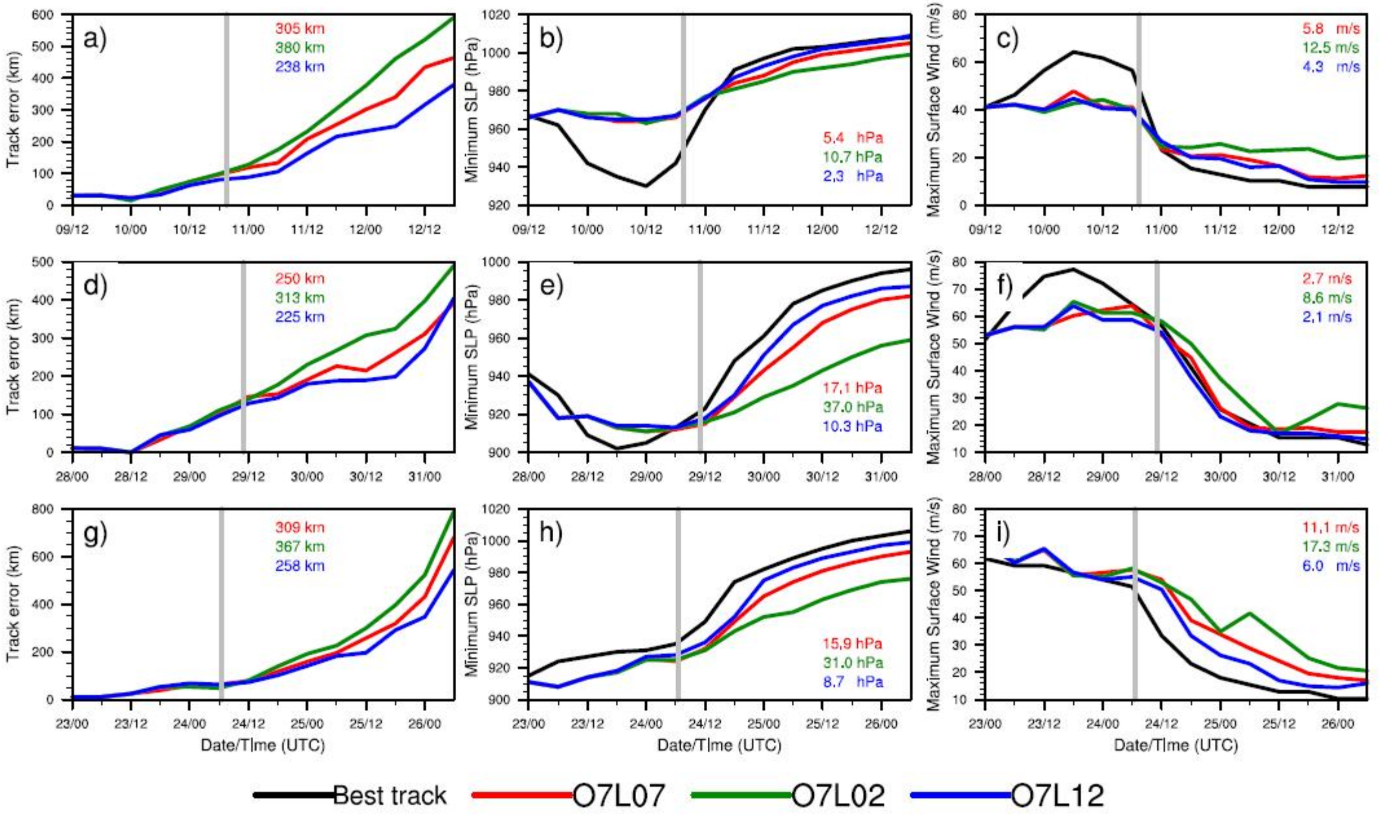

The boundary layer scheme has a significant impact on the simulated typhoon track, surface wind speed and pressure, and the core (e.g., Braun and Tao, 2000; Fang et al, 2009; Nolan et al, 2009a, b; Zhang et al, 2017, et. al.）

Problems faced in typhoon atmospheric boundary layer parameterization

Commonly-used parameterization schemes developed for general convective boundary layers

It is difficult to observe the violent boundary layer of typhoons. The rare typhoon boundary layer observations were taken from the low wind speed area in outer-core of typhoon.

2. Measurements and methods

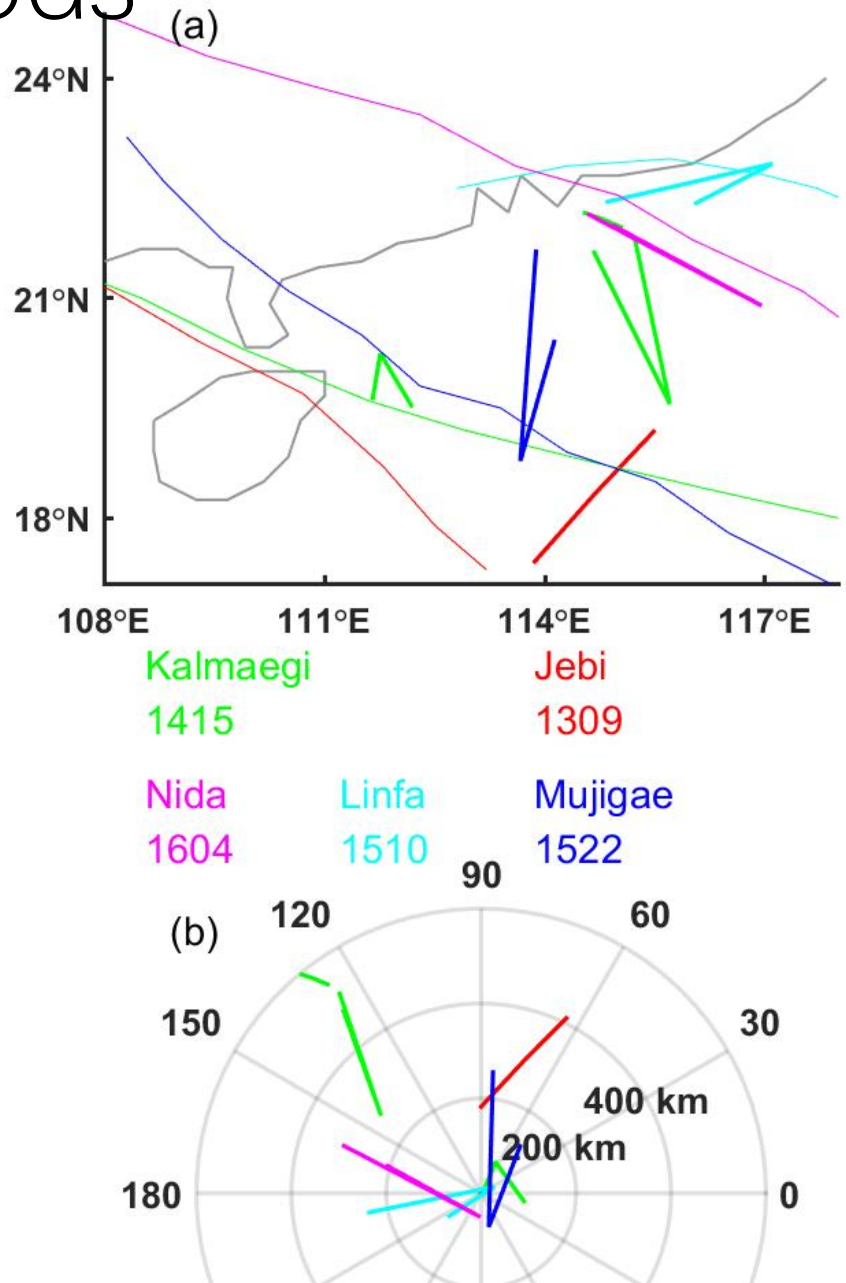

AIMMS-20 Data Specification

	Range	Accuracy	Resolution
Horizontal wind (u and v)	0 – ± 90 m/s	<= 1 m/s	0.1 m/s
Pressure	500 – 1040 hPa	1 hPa	0.1 hPa
Temperature	-20 – 50 degree Celsius	0.3 degree Celsius	0.1 degree Celsius
RH	0 – 100 %	3 %	1 %

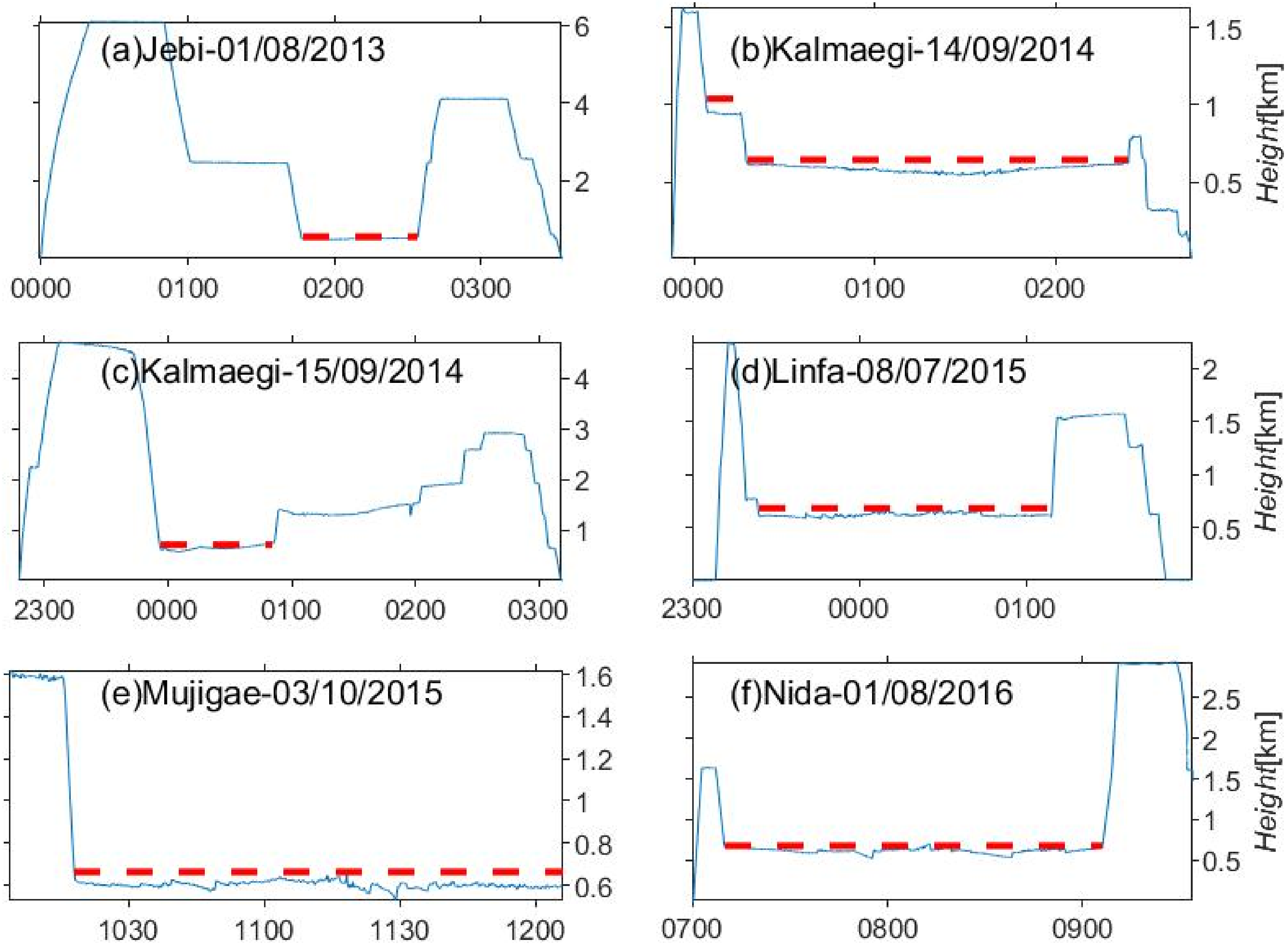

(a)Jebi-01/08/2013
(b)Kalmaegi-14/09/2014
(c)Kalmaegi-15/09/2014
(d)Linfa-08/07/2015
(e)Mujigae-03/10/2015
(f)Nida-01/08/2016
Height[km]
Height[km]
Height[km]
0000
0100
0200
0300
2300
1030
1100
1130
1200
0700
0800
0900

Quality control

- A turbulence spectrum of slope −5/3 check,
- A turbulence stationarity check,
- A cumulative spectrum stabilization check

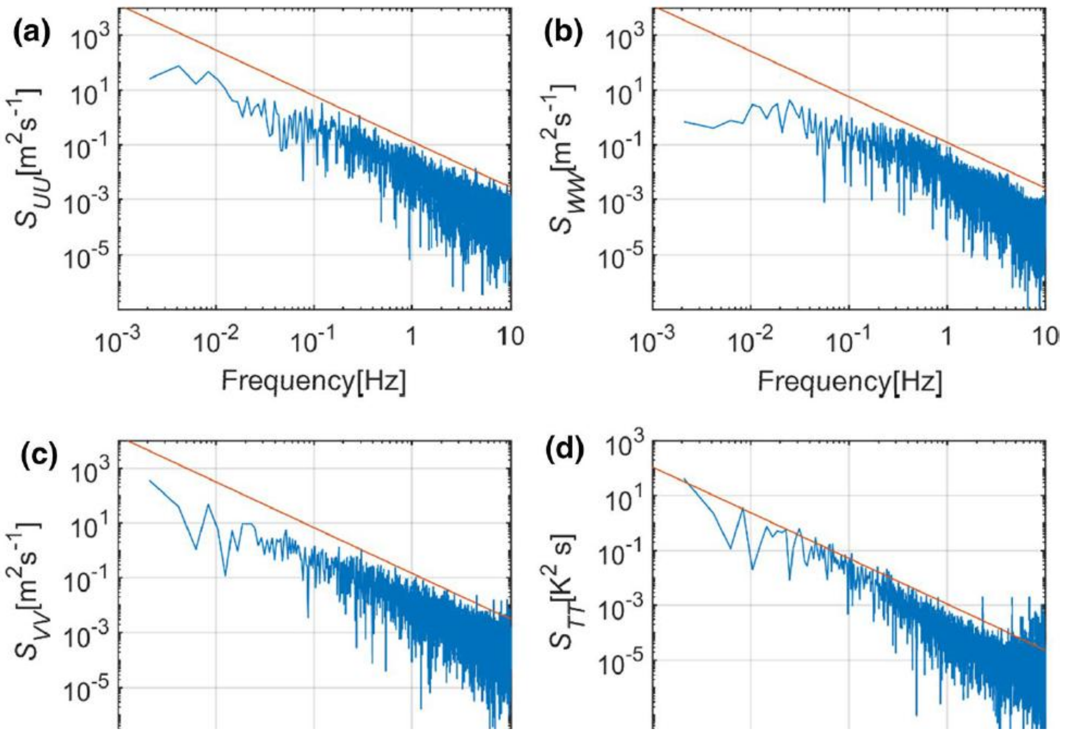

20150708-LINFA-20Hz

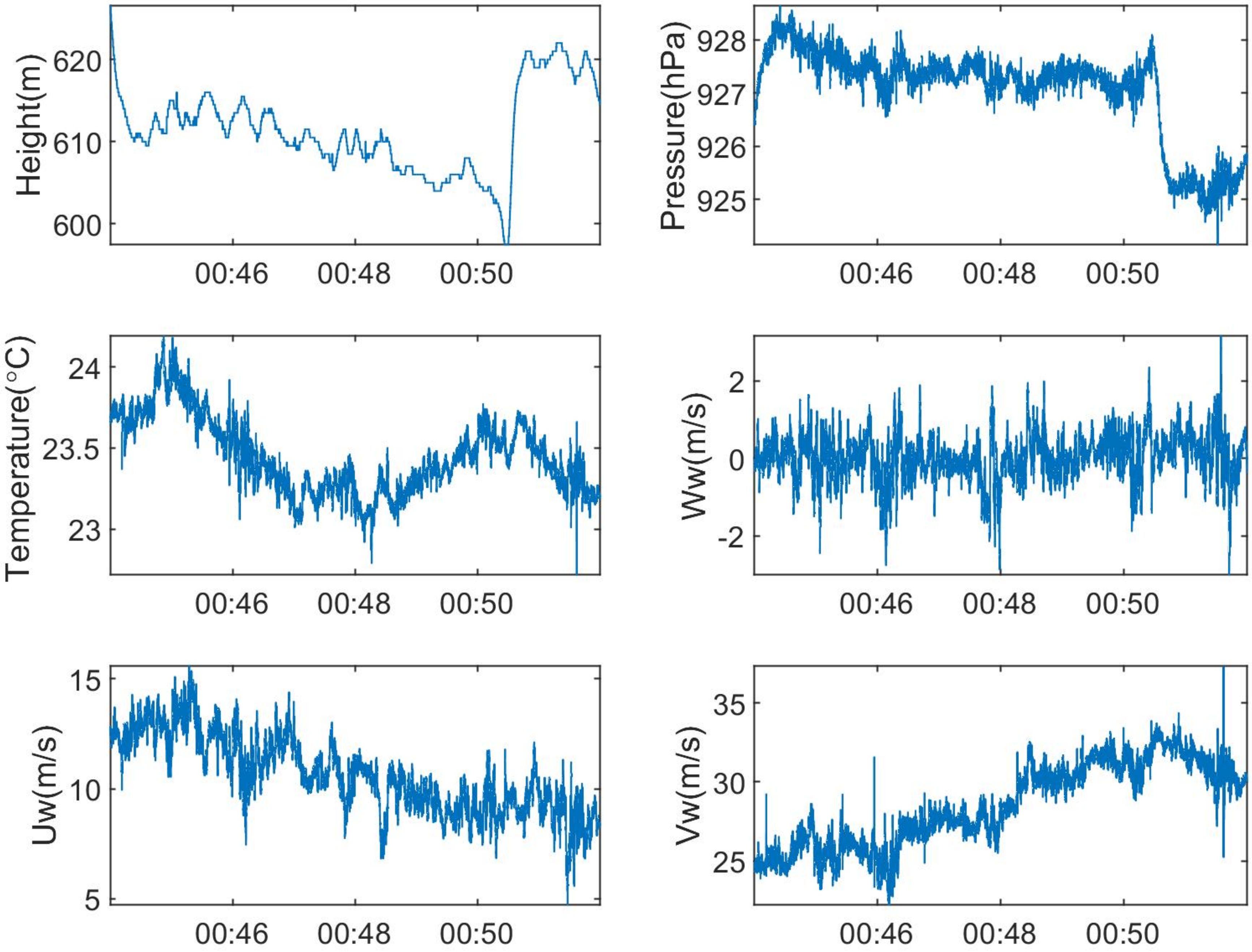

Methods of estimating vertical diffusivity K_m: standard deviation of vertical velocity and turbulence kinematic energy

The calculation of the turbulence kinetic energy (TKE, e) was based on

$$e = 0.5(\overline{u'^2} + \overline{v'^2} + \overline{w'^2}). \tag{3}$$

According to the two parametrization schemes commonly used in a tropical cyclone model (Wang 2001), the Hanna method (Hanna 1968) and a method using the TKE and its dissipation rate (Holt and Raman 1988), we can estimate the vertical eddy diffusivity. Using the Hanna method (Hanna 1968), the eddy diffusivity K_1 can be estimated using

$$K_1 = cl\sigma_w, \tag{4}$$

where the constant $c = 0.41$ (Nieuwstadt 1984), σ_w corresponds to the standard deviation of the vertical velocity, l is the vertical mixing length

$$l = \sigma_w^3/\varepsilon, \tag{5}$$

and ε is the dissipation rate, which can be related to turbulence energy within the inertial subrange by

$$\varepsilon = \frac{2\pi}{U_{TAS}}\left[\overline{f^{5/3}S(f)}/\alpha\right]^{3/2}, \tag{6}$$

where f is the frequency, U_{TAS} is the true airspeed with respect to the aircraft, α is the Kolmogorov constant ($\alpha = 0.52$), and $S(f)$ is the frequency-dependent power spectral density

The eddy diffusivity, as estimated using TKE and its dissipation rate (Holt and Raman 1988), corresponds to

$$K_2 = c_2 e^2/\varepsilon, \tag{7}$$

where the constant $c_2 = 0.07$ (Zhang and Drennan 2012).

Results

Scale analysis: co-spectrums and their ogives (frequency cumulative)

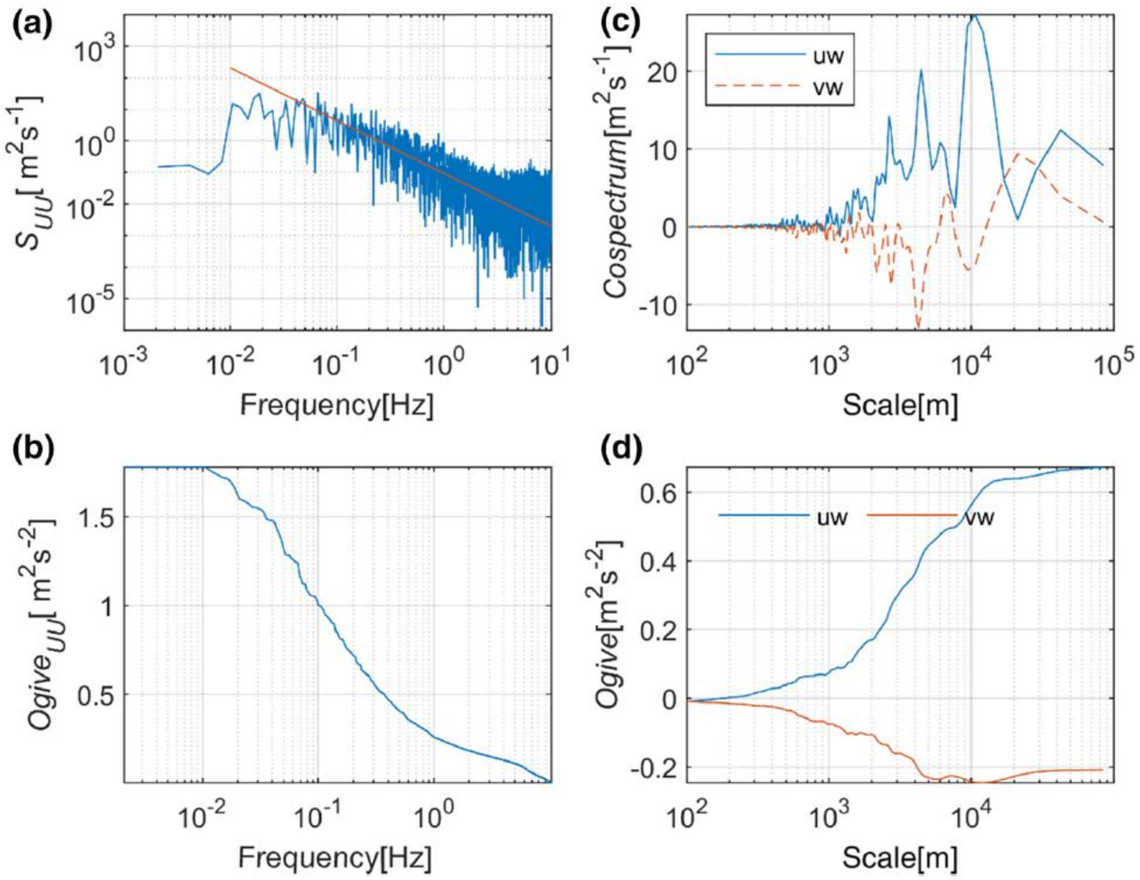

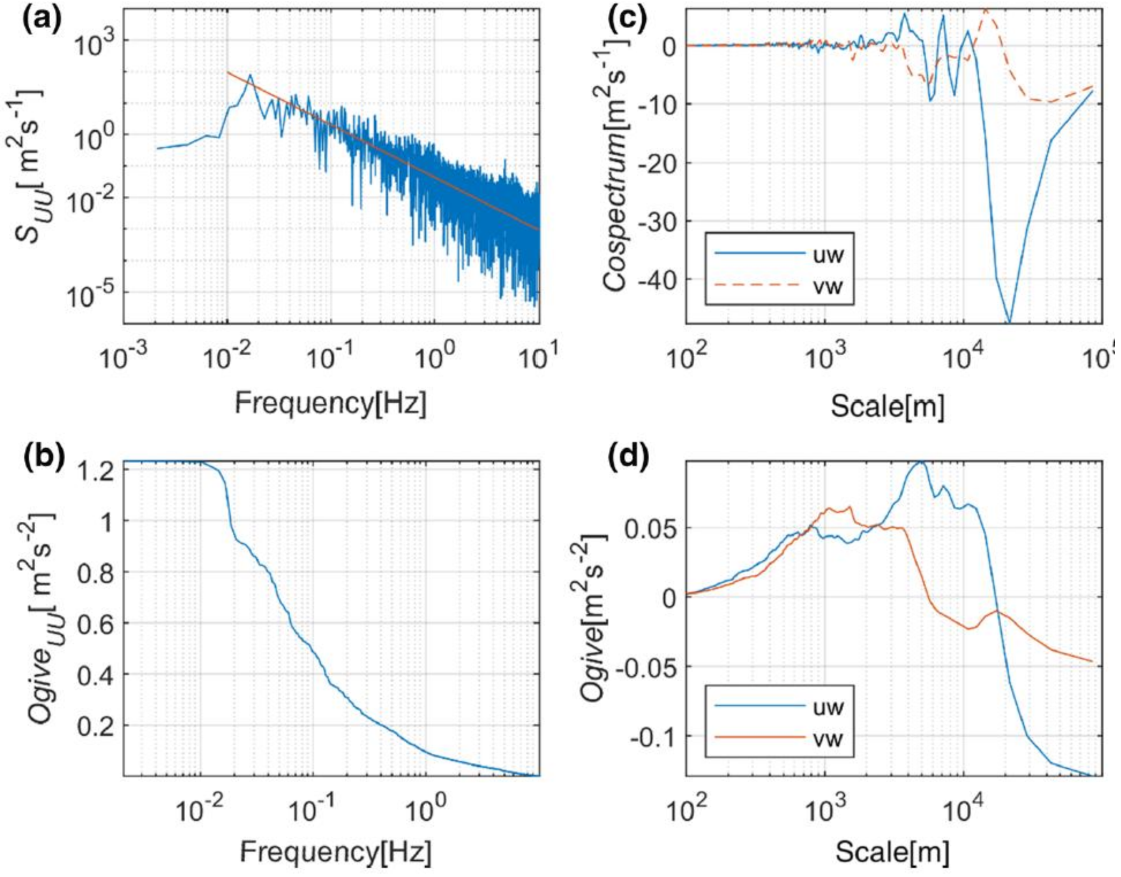

Eddies with horizontal scale<10 km, occupied ~85% of the samples

Eddies with horizontal scale >10 km

Larger-scale eddies are related to fine-scale spiral rainbands

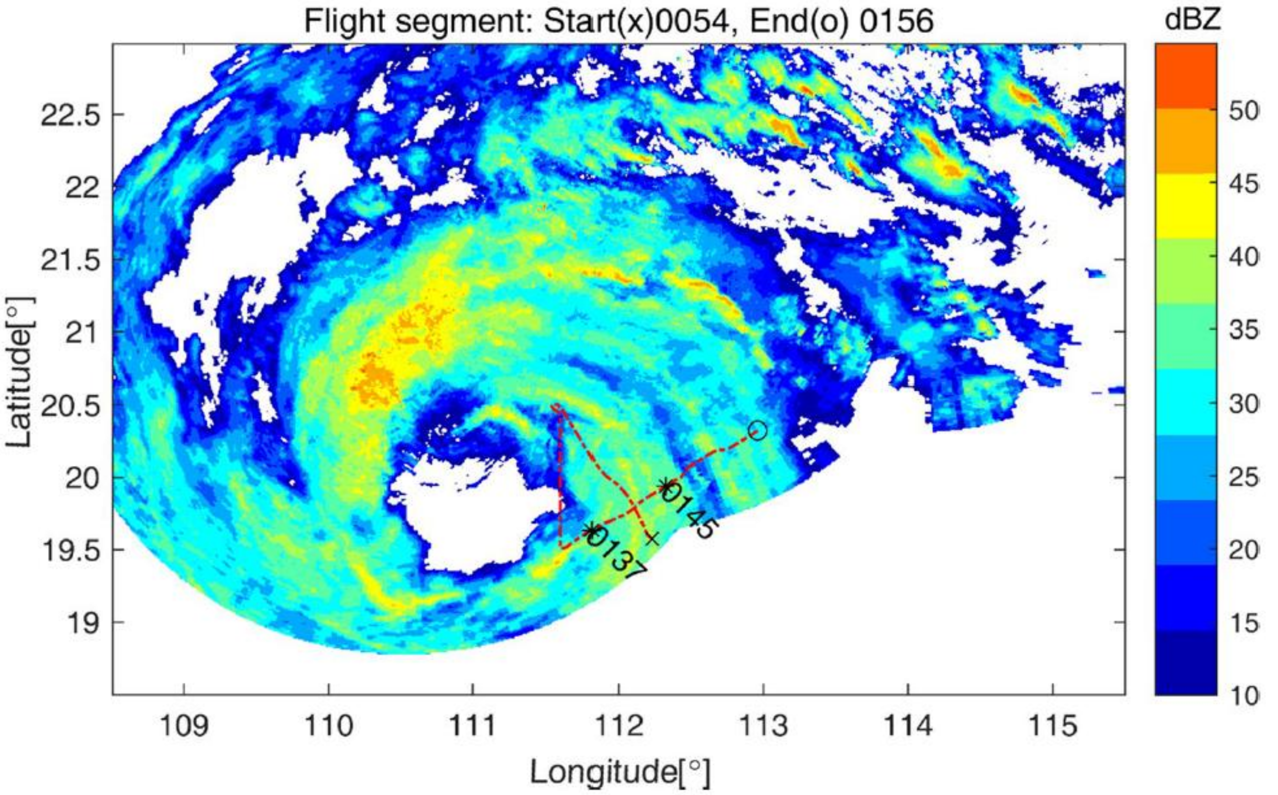

Fig. 6 The projection of the flight segment during Kalmaegi (1415) on the composite radar reflectivity at a height of 3 km at 0124 UTC on 15 September 2014 from the South China weather radar network. The start

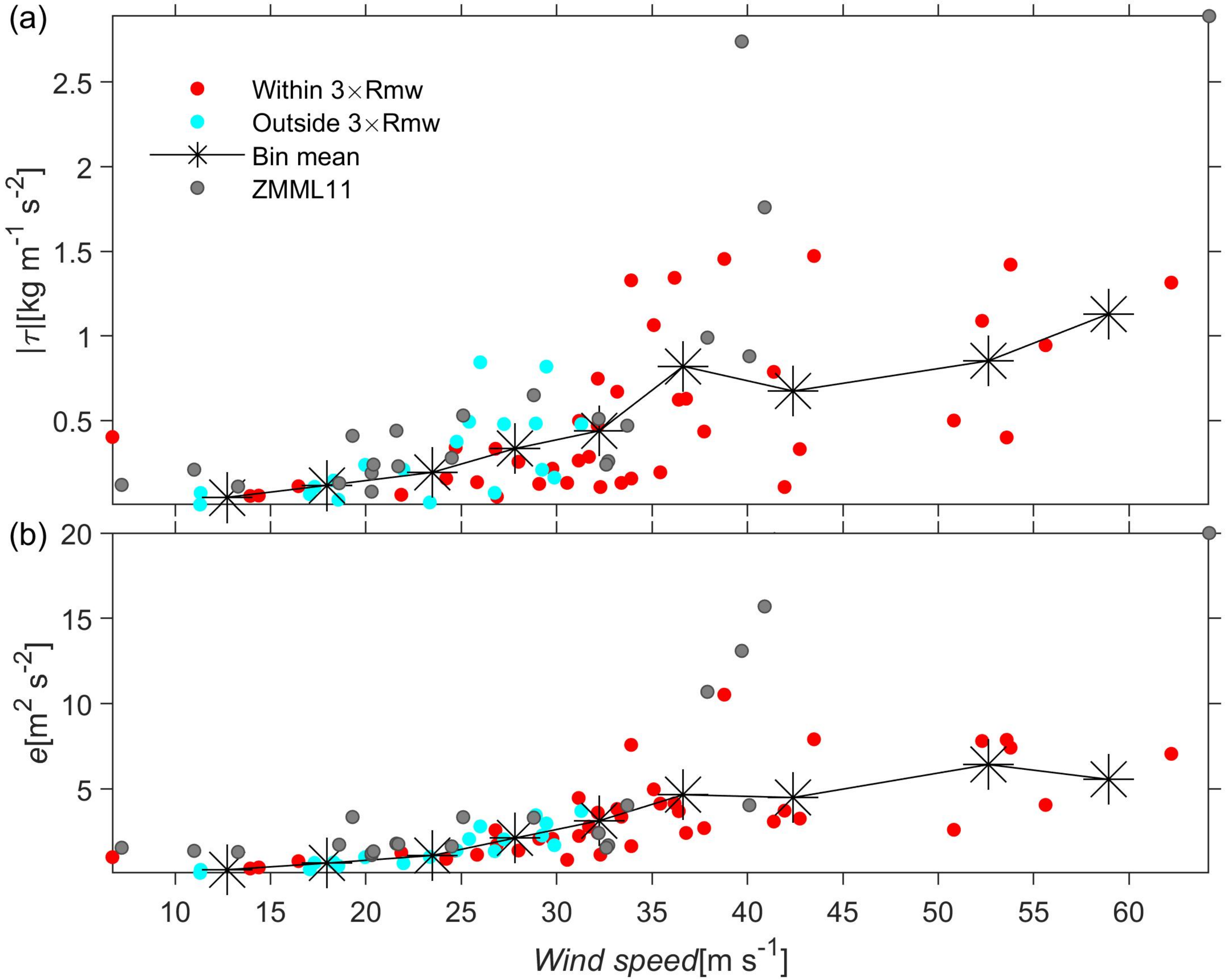

(a)
(b)
Within 3×Rmw
Outside 3×Rmw
Bin mean
ZMML11
|τ|[kg m^-1 s^-2]
e[m^2 s^-2]
2.5
2
1.5
1
0.5
20
15
10
5
10 15 20 25 30 35 40 45 50 55 60
Wind speed[m s^-1]

Projection of the fight path on the composite radar reflectivity during typhoon Nida in 2016

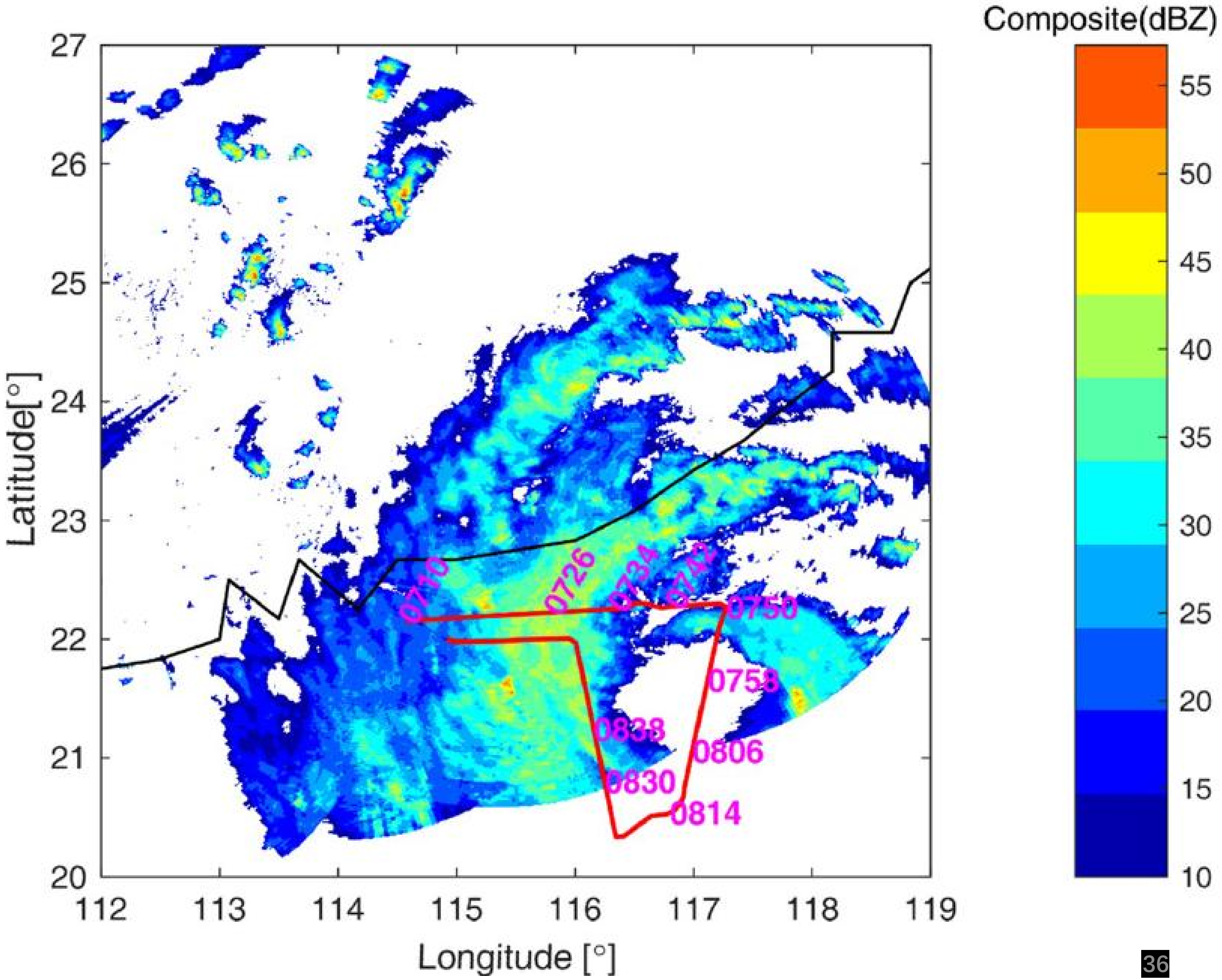

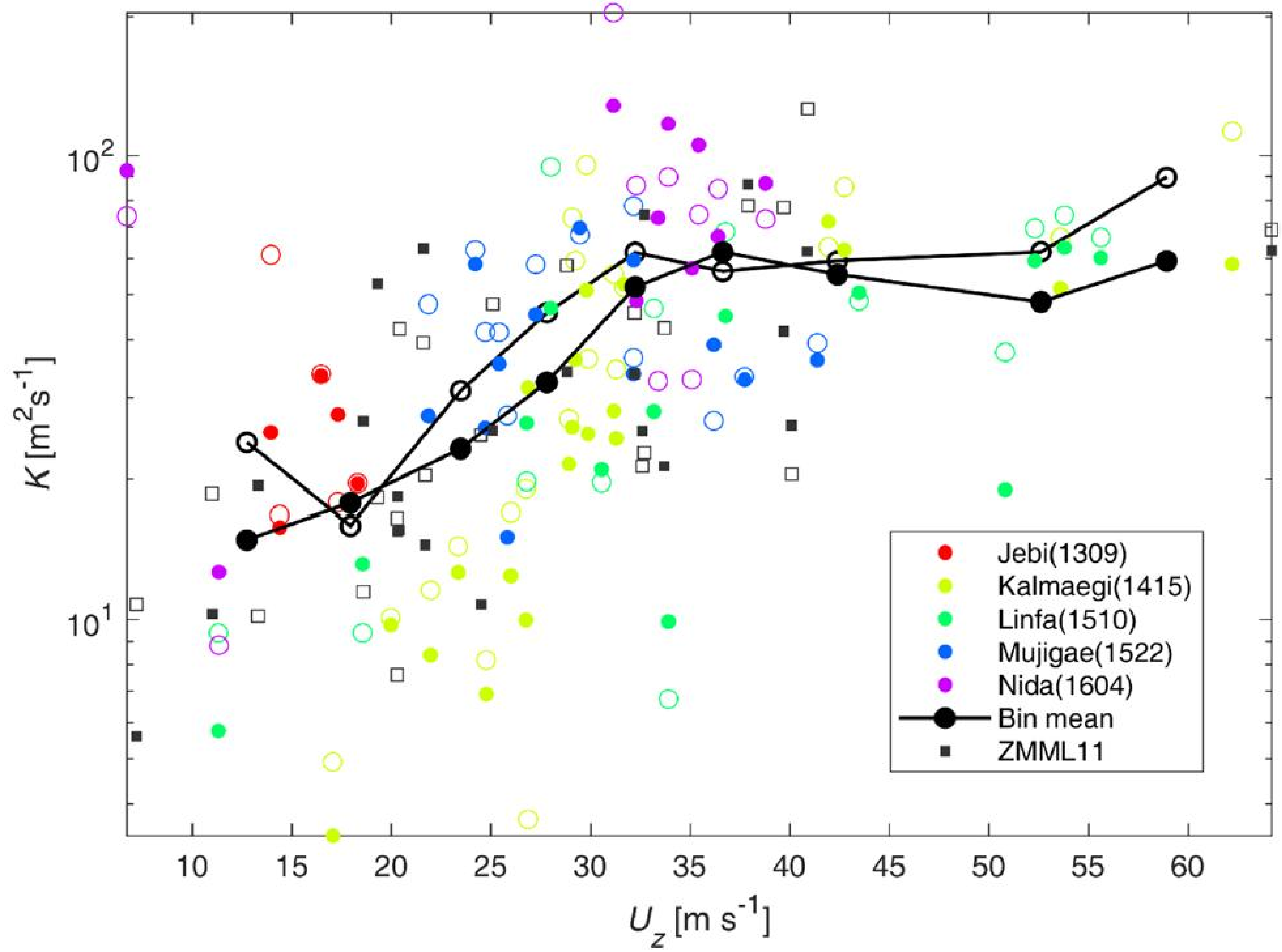

10^2
10^1
K [$m^2 s^{-1}$]
10
15
20
25
30
35
40
45
50
55
60
U_z [m s^{-1}]
Jebi(1309)
Kalmaegi(1415)
Linfa(1510)
Mujigae(1522)
Nida(1604)
Bin mean
ZMML11

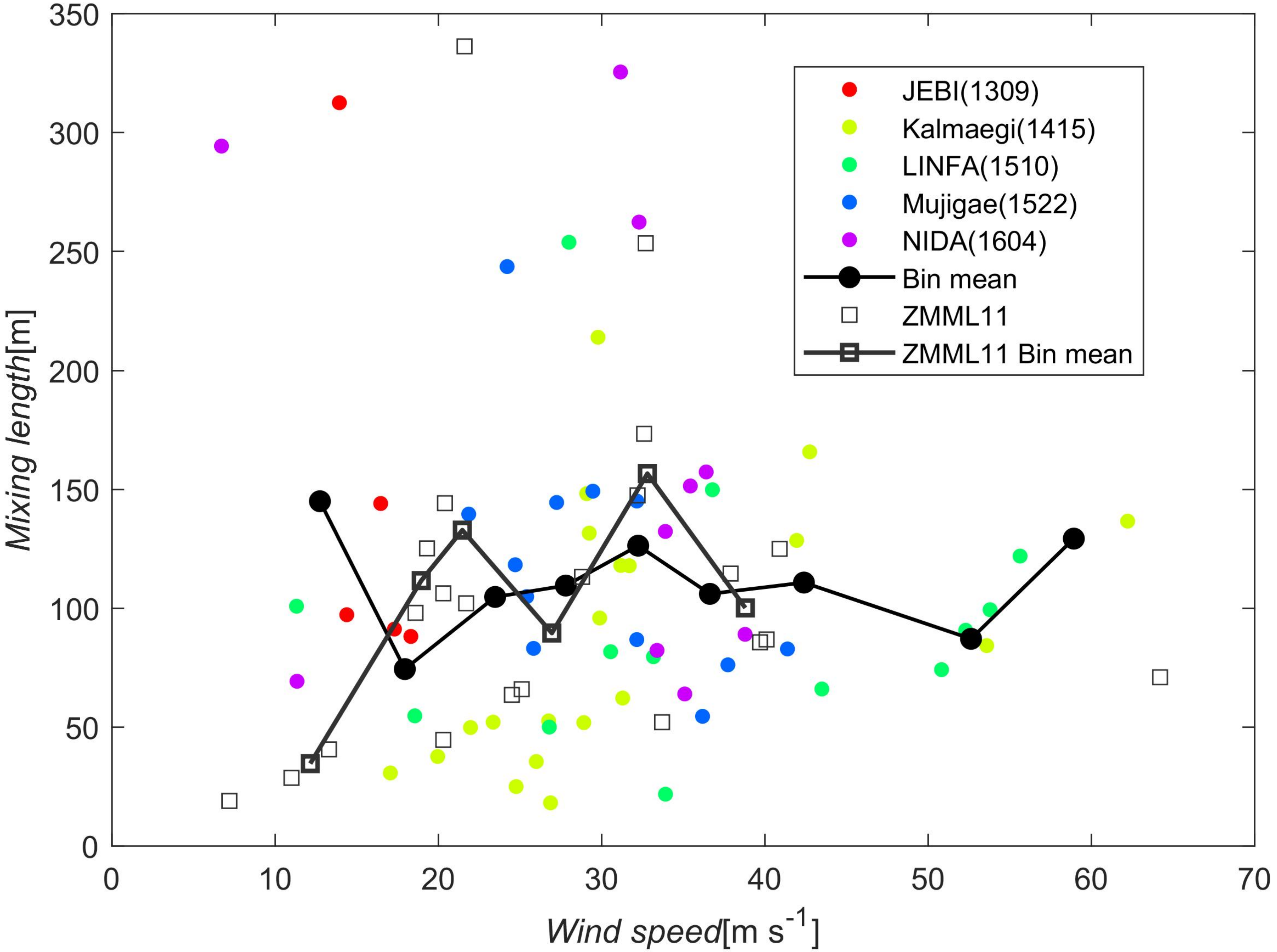
JEBI(1309)
Kalmaegi(1415)
LINFA(1510)
Mujigae(1522)
NIDA(1604)
Bin mean
ZMML11
ZMML11 Bin mean
Mixing length[m]
Wind speed[m s-1]
0
50
100
150
200
250
300
350
0
10
20
30
40
50
60
70

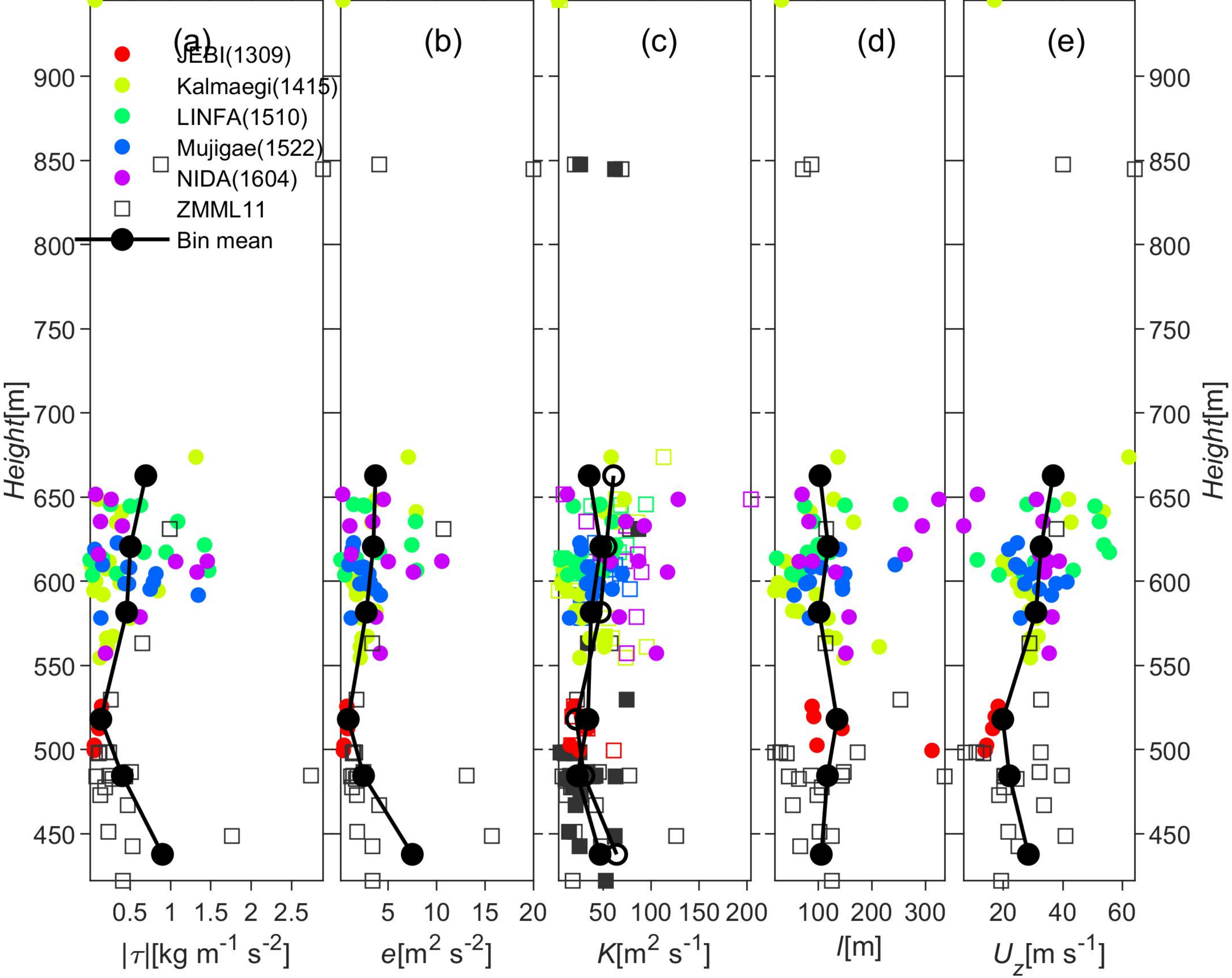

(a)
(b)
(c)
(d)
(e)
JEBI(1309)
Kalmaegi(1415)
LINFA(1510)
Mujigae(1522)
NIDA(1604)
ZMML11
Bin mean
Height[m]
|τ|[kg m-1 s-2]
e[m2 s-2]
K[m2 s-1]
l[m]
Uz[m s-1]

Parameterization of vertical diffusivity K_m

$$K = \kappa u_{*s} z(1 - z/h)^p,$$

$$u_*^2 = u_{*s}^2 - A f_c z u_{*s},$$

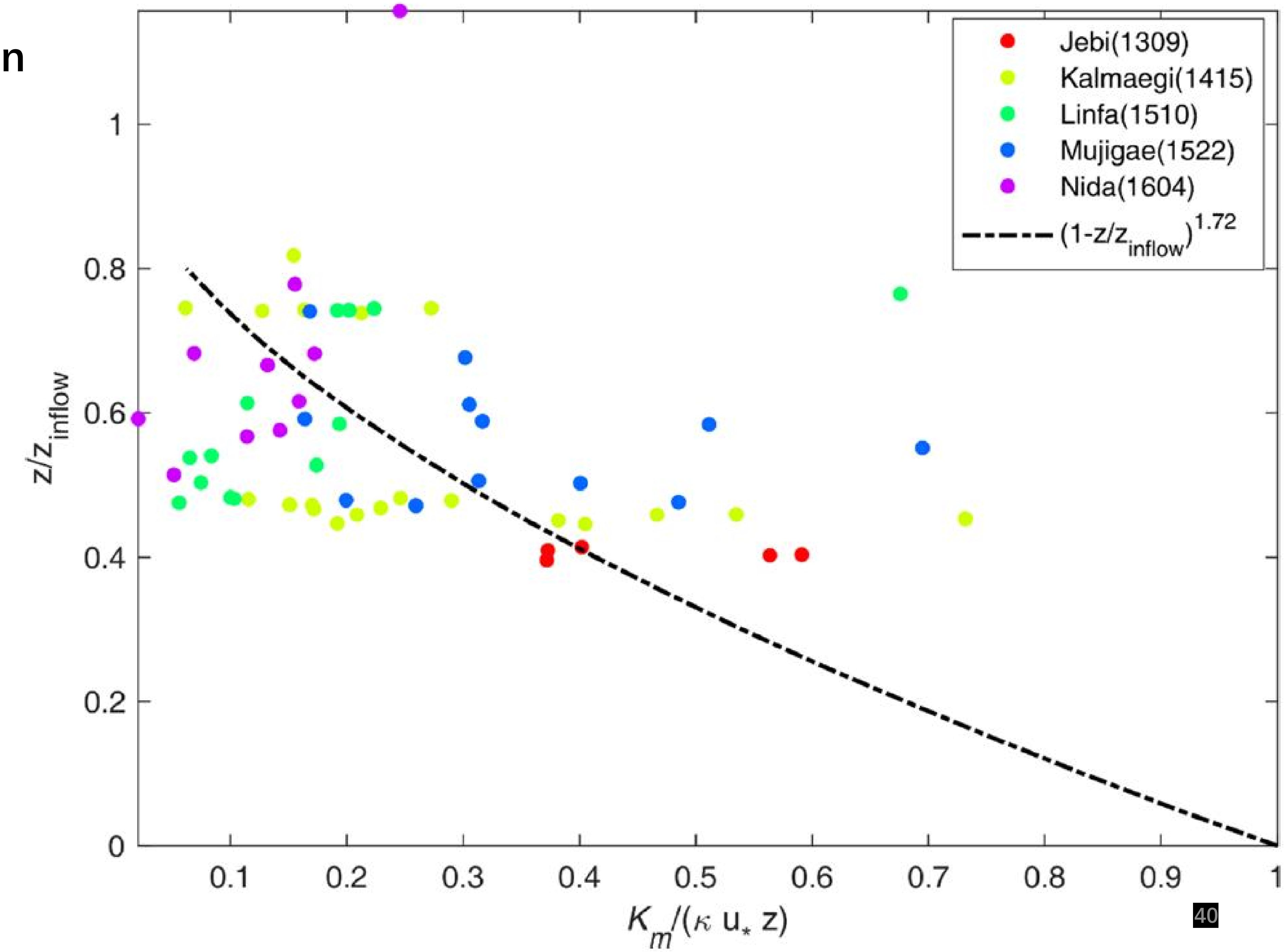

Discussion and conclusions

- Atmospheric boundary layer observation data from Hong Kong Observatory aircraft during five typhoons in the northern South China Sea. The observation altitude range was 500-700 m, and the distance from the typhoon center was 0-600km (including observations through the eye wall); scale analysis showed that 85% of sample turbulent vortices were The horizontal scale is 1-10 km, and the turbulent flux mainly comes from turbulent eddies with a horizontal scale below 5 km.
- In the wind speed range of 10-36 m/s, the momentum flux and TKE increase with the increase of wind speed; in the higher wind speed range (<62 m/s), the increase of these two quantities with wind speed weaken significantly.
- The vertical eddy diffusion coefficient K_m estimated by the vertical velocity are in good agreement with those estimated by the TKE method; in the wind speed range of 10-36 m/s, K_m increases with the increase of wind speed, from 10 m2/s to 60-70 m2/s; under higher wind speed conditions, K_m tends to level-off. The dependence of mixing length on wind speed is not significant, with an average value of approximately 100 m.
- The large eddy diffusion coefficient of the typhoon eyewall is worth noting (~100 m2/s)